The role that myeloid protein tyrosine phosphatase 1B (PTP1B) plays in obesity and type 2 diabetes with focus on neuroinflammation

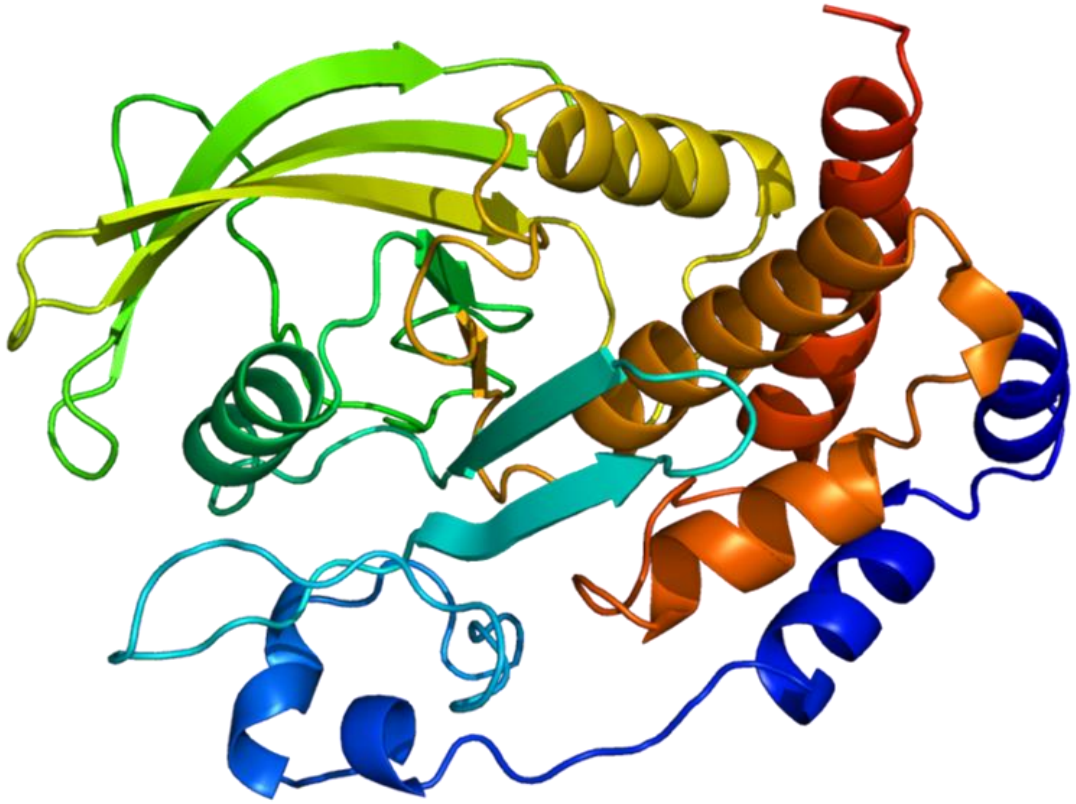

Final thesis
Major Project
Tom Metz
August 2015

Supervisors
Dr Delibegovic
Dr Eggen

University of Aberdeen
Rijksuniversiteit Groningen

Behavioural and Cognitive Neurosciences (BCN)
Molecular and Clinical Neuroscience (N-track)

-Abstract-

Obesity and diabetes are a major health concern in the Western world. Protein tyrosine phosphatase-1B (PTP1B) is an attractive drug target for obesity and type 2 diabetes (T2D); it is known to negatively regulate both the insulin receptor and the leptin receptor. Mice lacking PTP1B are protected from diet induced insulin resistance and obesity. However, due to the potential anti-inflammatory role of PTP1B, investigation into the role of PTP1B in the immune system is needed. Microglia have been shown to be both increased in number and in activation in several disease states, such as stroke, dementia, depression and obesity. LysM is expressed in microglia, which are inflammatory cells in the central nervous system. Therefore the role of PTP1B in hypothalamic inflammation and whole-body metabolism was assessed using myeloid cell PTP1B knockout mice (Lysm-PTP1B) on either regular chow diet or high fat diet. Our aim was to investigate the role of myeloid PTP1B in obesity. Our research shows that high-fat feeding leads to increased serum leptin and insulin levels and these levels are reduced again in Lysm-PTP1B mice. However, the lack of myeloid PTP1B does not reduce the increased body weight of mice on high-fat diet. The Lysm-PTP1B mice are protected against ER-stress, but the increase in ER-stress under high-fat diet conditions cannot be reduced. Messenger RNA of several inflammatory mediators could not be detected in the hypothalamus. Strikingly, microglial inflammation markers are increased in high fat diet mice, but only in the knock-out group. This research indicates that inhibiting myeloid PTP1B restores serum insulin and leptin levels and might act through lowering hypothalamic ER-stress.

Table of contents

1. Introduction

There has been a major increase in obesity in the Western society over the last couple of decades[1]. Obesity is a chronic condition characterized by excess fat deposition in organs, such as adipose tissue, liver, skeletal muscle, heart, and pancreatic islets, which affects the quality of life and reduces life expectancy[2]. The harmful effects of obesity are due to its association with diseases including type 2 diabetes (T2D), atherosclerosis, non-alcoholic steatohepatitis, hypertension, certain types of cancer, and joint and bone disorders[2]. The increase in consumption of energy rich foods and a reduction in physical activity, which are changes in lifestyle over the last decades, are generally considered to be main causes for the high prevalence of obesity. An indicator of the degree of obesity is the body mass index (BMI), which is calculated by *BMI=body weight/height^2* with body weight measured in kilograms and height measured in meters. A BMI higher than 25 indicates that someone is overweight and a BMI over 30 indicates that someone is obese. In Western Europe over 20% of the adult population is obese (Netherlands: 12.7% in men and 15.9% in women; UK: 24.5% in men and 25.4% in women) and more than 50% of the population is overweight[3]. Epidemiological studies indicate an expected growth of the number of people suffering from obesity worldwide over the next 15 years[4]. Obesity is caused by an imbalance in energy homeostasis and the main regulator of energy homeostasis is the hypothalamus[5]. Leptin and insulin are the two most important agents influencing the hypothalamus and their signalling is essential in keeping the energy homeostasis in balance. High-fat feeding affects insulin and leptin signalling, contributing to dysregulation of hypothalamic energy homeostasis[6]. The global increase in obesity seems to go hand in hand with an increase in T2D[1]. In T2D, higher insulin levels do not lead to a normal response anymore, indicating that there is something wrong with the insulin signalling. Obesity and over-nutrition are associated with an increased risk of diabetes[5], but the mechanisms behind this are not completely understood yet. Possible mechanisms contributing to obesity and T2D are insulin resistance (IR)[7] and leptin resistance (LR)[8]. Other mechanisms that have been linked with obesity and T2D are inflammation[9] and endoplasmic reticulum (ER) stress[10]. Recent research has indicated protein tyrosine phosphatase 1B (PTP1B) as a possible target for the development of therapeutic agents against T2D[11]. PTP1B inhibits both insulin and leptin signalling[11] and is therefore believed to reduce the insulin and leptin resistance leading up to T2D. The involvement of PTP1B in ER-stress[12] and inflammation[13], makes it a very interesting target for therapy against T2D. Mice lacking PTP1B have already shown to be protected from diet induced insulin resistance and obesity[14,15]. These mice have lower levels of glucose and insulin in the blood and increased phosphorylation of the InsR[15]. The PTP1B$^{-/-}$ mice also showed decreased adiposity due to reduced fat cell mass, increased insulin-mediated glucose disposal, and increased energy expenditure[14]. Klaman et al. were the first to suggest that insulin sensitivity in PTP1B$^{-/-}$ mice is tissue specific; skeletal muscle was more insulin sensitive, while adipose tissue was not affected[14]. This has been further investigated in several different tissue specific PTP1B knock-out models[11,16-18]. The role of PTP1B in neuroinflammation has not yet been studied extensively. Obesity is associated with an

increase in inflammation in the hypothalamus[19]. Infiltration of microglia is observed in the hypothalamus of obese humans as well as animal models of obesity[19]. This indicates that obesity is related to neuronal injury in a brain area crucial for body weight control. The increased expression of PTP1B is one of the key molecular mechanisms known to play a role in the induction of hypothalamic leptin and insulin resistance[20]. Previous research has indicated that deletion of PTP1B in myeloid cells leads to a decrease in inflammation and an increase in insulin sensitivity[13]. Microglia have been shown to be both increased in number and in activation in several disease states, such as stroke, dementia, depression and obesity[21], indicating the presence of neuroinflammation in those disease states. Microglia cells can be seen as the main regulators of neuroinflammation. In the current study, the effects of the deletion of PTP1B in microglia will be tested. Insulin and leptin signalling will be measured, along with inflammatory and ER-stress markers. The inhibition of PTP1B is a potential anti-inflammatory and anti-diabetic target in obesity.

1.1 Neuroinflammation

Neuroinflammation is mediated mainly by microglia, the immune cells of the central nervous system (CNS). Microglia activation can be caused by neuronal injury or invading pathogens and is characterised by the migration of microglia to the site of injury and the engulfment of dead or pathogenic cells and cell debris. Under physiological conditions microglia are in a resting or "ramified" state, they are highly branched and continuously scanning their surroundings. Activation of the microglia comes along with morphological changes, the "ramified microglia" change into "amoeboid microglia" so that they can easily migrate to the site of injury[22]. Activated microglia and damaged neuronal cells release pro-inflammatory mediators, such as nitric oxide (NO), inducible NO synthase (iNOS), interleukin-1β (IL-1β), interleukin-6 (IL-6), and tumour necrosis factor-α (TNF-α), that help coordinate the local and systemic inflammatory response to pathogens and damage. In contrast, microglia also produce anti-inflammatory cytokines, such as interleukin-10 (IL-10) and interleukin-4 (IL-4), when activated. These cytokines work against the inflammatory response to maintain the homeostasis of the overall immune response. The activation of microglia protects the brain against further damage from pathology. However, chronic and excessive microglial activation can be toxic and may play an important role in the pathogenesis of different neurodegenerative diseases such as Parkinson's disease (PD)[23], Alzheimer's disease (AD)[24], and multiple sclerosis (MS)[25], and neurological diseases like depression[26], but also in obesity and T2D[19].

1.2 Type 2 diabetes (T2D)

The characterization of T2D is the high levels of glucose in the blood. In the normal human body, β-cells on the Islets of Langerhans of the pancreas produce insulin in response to a rise in serum glucose, for instance after a meal. In order to be used by the cells of the body, glucose must be transported across the plasma membrane of the cell by glucose transporters. In all cells of the body, except for neurons, the insertion of

glucose transporters into the membrane occurs when insulin binds to insulin receptors on the cell surface[27]. Therefore, a rise in serum glucose must be accompanied by a rise in insulin, for the glucose to be utilized or stored by the cells in the body. Diabetes mellitus is a condition characterized by high blood glucose levels. Lack of insulin signalling causes the hyperglycaemia, because the glucose absorbed from the intestines cannot be taken up by the cells of the body (except neurons). The excess glucose passes to the urine, making it sweet. But the excess glucose also causes major health issues, both acute and chronic. In people with type 1 diabetes, β-cells are destroyed due to autoimmunity and insulin is not produced, leading to hyperglycaemia[28]. Type 1 diabetes can nowadays be controlled quite well, by injecting insulin. The hyperglycaemia in T2D has a different cause, because the β-cells are initially still intact and insulin is produced. Insulin injection does not effectively help patients with T2D, because insulin is not as efficient at its job. However most diabetics do end up on exogenous insulin because nothing else works. There are no good insulin sensitizers, apart from metformin, which often has to be given in a combination with other drugs. Metformin decreases hepatic glucose production and improves insulin sensitivity by increasing glucose uptake in the peripheral tissues. Combination of canagliflozin and metformin is one of the newest combination therapies available for the treatment of T2D[29]. Canagliflozin inhibits the sodium-glucose co-transporter 2 which causes a decrease in reabsorption of glucose and therefore an increase in the urinary excretion of glucose[29]. This seems to be an effective method of lowering blood glucose levels in patients with moderate T2D. However, there are also side effects, like genital mycotic infections and hypotension[29]. Moreover, this kind of medication treats the consequences of T2D, but it does not restore the balance in the metabolism of the patient.

The mechanism believed to underlie T2D is insulin resistance[30]. The major risk factor for insulin resistance is being overweight[31], which can explain the link between obesity and T2D. Insulin resistance causes β-cells to increase insulin production, which causes hyperinsulinemia[32]. This mechanism will initially keep the blood glucose at normal levels, but when β-cell function begins to decline, the insulin production is inadequate to overcome the rise in blood glucose levels, resulting in hyperglycaemia.

So far T2D has been a chronic disease and is associated with increased risk of cardiovascular diseases, lower limb amputations, blindness, kidney failure and ultimately leads to an earlier death[33]. It has also been associated with an increased risk of cognitive dysfunction and dementia through disease processes such as Alzheimer's disease and vascular dementia[34]. It is therefore of great importance that T2D becomes reversible and no longer has to be a chronic disease.

1.3 PTP1B and its role in metabolic regulation

The current treatments available for T2D have been focussed on exercise and dietary management of obesity to improve insulin sensitivity, to increase insulin secretion, and to inhibit or reduce the rate of glucose absorption from the gut. So far, medications for T2D include biguanides, sulfonylureas, α-glucosidase inhibitors and

thiazolidinediones[35]. However, there are many shortcomings in the clinical use, because these drugs are designed for symptoms not for disease target. Recently, PTP1B has emerged as promising therapeutic target for the treatment of T2D[11].

PTP1B is a protein that is part of a family of proteins (PTPs) which are responsible for tyrosine phosphorylation and dephosphorylation. Tyrosine phosphorylation of proteins is a fundamental mechanism for the control of cell growth and differentiation. Protein tyrosine kinases (PTKs) and protein tyrosine phosphatases (PTPs) are responsible for phosphorylation and dephosphorylation, respectively, and are therefore the two main regulatory mechanisms for tyrosine phosphorylation[36]. Disturbed activity of PTPs or PTKs leads to abnormal tyrosine phosphorylation, and contributes to the development of many diseases like diabetes, cancer and inflammatory disorders[37].

PTP1B is an intracellular PTP and has been identified as an attractive drug target for obesity and diabetes[38]. PTP1B is a non-receptor tyrosine phosphatase involved in regulation of various cell signalling cascades, including the leptin and insulin pathways (fig. 1[35]).

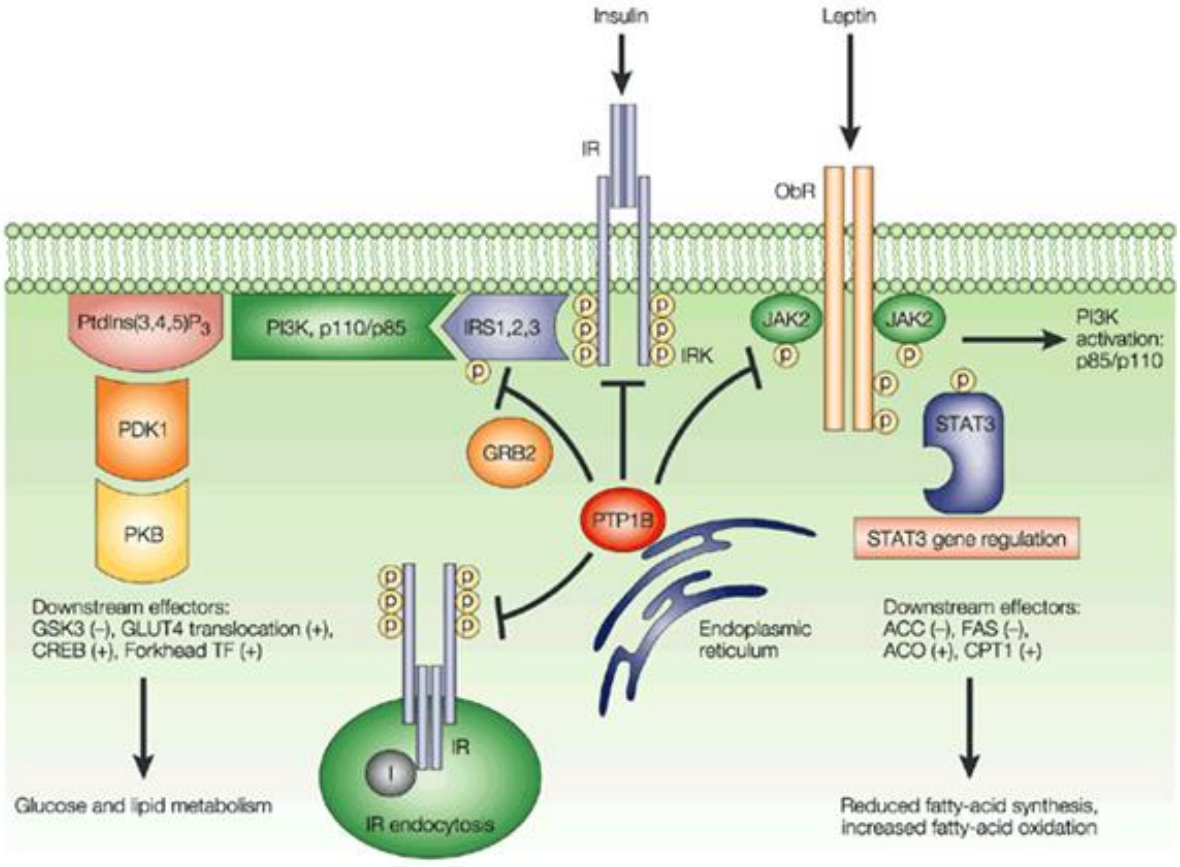

Figure 1: Regulation of insulin and leptin signalling by PTP1B[35]

1.3.1 Role of PTP1B in insulin signalling

Disturbed insulin signalling is an important mechanism in the development of T2D. Besides the peripheral activity, insulin also controls body weight through the central nervous system (CNS)[39]. Insulin receptors (InsRs) are present throughout the CNS. In rodents, the highest density of InsRs is found in the olfactory bulb, hypothalamus, cerebral cortex, cerebellum, hippocampus, thalamus, and midbrain[40]. Insulin can enter the brain from the circulation through insulin receptors expressed on endothelial cells in the blood-brain barrier, which transport insulin trough the endothelial cells into the brain[41]. Inside the brain insulin can bind and activate its receptors[42,43]. IRs are tetrameric membrane receptors composed of two extracellular α subunits and two transmembrane β subunits[44]. Insulin binds to the extracellular subunits that activate the tyrosine kinase activity on the β subunits, which activates the insulin receptor substrate (IRS)[45]. The phosphorylation of the IRS then leads to the activation of two major signalling pathways: 1) the mitogen-activated protein kinase (MAPK) cascade and 2) the phosphoinositide 3 kinase (PI3K) pathway[44]. Both these pathways, but mainly the PI3K pathway, are regulators of food intake and hepatic glucose production[44]. Downstream of PI3K, protein kinase B (PKB; also known as AKT) is triggered, which activates subsequent translocation of the glucose transporter GLUT4 and lowers blood glucose levels by inducing glucose uptake in muscle and inactivation of glycogen-synthase kinase 3 (GSK3)[46]. The inhibition of insulin signalling by PTP1B therefore leads to an increase in serum glucose; inhibition of PTP1B can restore these levels again.

1.3.2 PTP1B in leptin signalling

Another essential hormone in human metabolism is leptin, the so called “satiety hormone”. Leptin is produced in adipose cells and production of leptin increases with increasing adiposity[47]. Leptin sends a signal to the brain to indicate that there is enough energy so food intake can be decreased and energy expenditure can be increased. Leptin signalling uses a different intracellular pathway than insulin. Leptin only works in the brain, in contrast with insulin which has a primary effect in the periphery. Leptin is released in the blood and binds to leptin receptors (LepRs) which are found in the arcuate nucleus of the hypothalamus[48].

Binding of leptin to its receptor leads to the activation of janus kinase 2 (Jak2), which phosphorylates itself as well as the tyrosine (Y) residues Y985 and Y1138 on the intracellular LepR part[49]. Concurrently, Jak2 phosphorylates the IRS-1, activating the PI3K pathway in the same way as insulin, described before[50]. Phosphorylated Y985 then acts like a docking site for SH2-containing protein-tyrosine phosphatase-2 (SHP2), which activates the extracellular signal regulated kinase (ERK) pathway[51]. The activated Y1138, on the other hand, recruits and activates signal transducer and activator of transcription 3 (STAT3)[49]. Leptin stimulates pro-opiomelanocortin (POMC) and inhibits AGRP through STAT3 signalling, while the inhibition of neuropeptide Y (NPY) is regulated through another leptin-dependent pathway[52]. Both POMC and NPY are important in regulating the body’s energy balance.

In obesity, leptin sensitivity is decreased, which leads to the inability to sense satiety despite high energy stores[53]. Leptin was marked as a potential cause of obesity when elevated levels of leptin were found in obese people[54], indicating that obese people are less sensitive to leptin. This effect is clearly demonstrated in the *db/db* mouse model, a model lacking LepRs[55]. Several mechanisms could be contributing to leptin resistance. Impaired leptin transport across the blood-brain barrier (BBB) could be indicated as a contributing factor to leptin resistance, since there are leptin receptors expressed on the endothelial cells of the BBB that act as leptin transporters[56]. Arguing for this theory is the fact that obese people have lower leptin levels in the CSF compared to the blood[57]. Another mechanism that potentially causes leptin resistance is reduced LepR signalling. Binding of leptin to the LepR activates several intracellular pathways, which lead to expression of proteins. One of the proteins expressed by leptin binding is suppressor of cytokine signalling-3 (SOCS-3), which normally inhibits further leptin signalling[58], creating a negative feedback loop. Excessive SOCS-3 activity could therefore, just like PTP1B, be a cause of LR.

Introduction of leptin in neuronal cells overexpressing the LepR in vitro has shown that PTP1B induces the dephosphorylation of JAK-2[20] (fig. 1). Deletion of PTP1B in mice has shown to have an increase in STAT3 phosphorylation after leptin injection[20], meaning that PTP1B$^{-/-}$ mice have a higher leptin sensitivity. Additionally, neuronal-PTP1B$^{-/-}$ mice have shown to have an increased hypothalamic leptin sensitivity[11]. This indicates that PTP1B deletion improves leptin signalling in the CNS as well as peripheral.

Insulin and leptin both bind to receptors on neurons in the arcuate nucleus of the hypothalamus and stimulate POMC and cocaine and amphetamine related transcript (CART) neurons, while inhibiting NPY and agouti-related peptide (AGRP) neurons (fig. 2[56]). NPY stimulates food intake[59], while melanocortins cleaved from POMC, such as α-MSH, lead to an inhibition of food intake[60]. The cleaved α-MSH binds to the melanocortin 4 receptor (MC4R). Other metabolic peptides, like ghrelin from the stomach and PYY form the gastrointestinal tract, also play a role in the balance between orexigenic and anorexigenic signalling. The orexigenic and anorexigenic signals from the arcuate nucleus project on the paraventricular nucleus (PVN), the lateral hypothalamic area (LHA) and the perifornical area (PFA), which connect to anabolic and catabolic pathways that connect to autonomic centres that process satiety and hunger signals[56]. In the nucleus of the solitary tract (NTS), signals from the hypothalamus are integrated with afferent input from liver and gastrointestinal tract transmitted through the vagus nerve and sympathetic nerves[56]. The different inputs come together to provide the overall balance between food intake and energy expenditure. The fact that PTP1B inhibits both insulin and leptin signalling makes that its presence in the hypothalamus has a huge impact on food intake and energy expenditure. The inhibition of PTP1B is therefore an important potential target to develop a therapy against obesity and T2D.

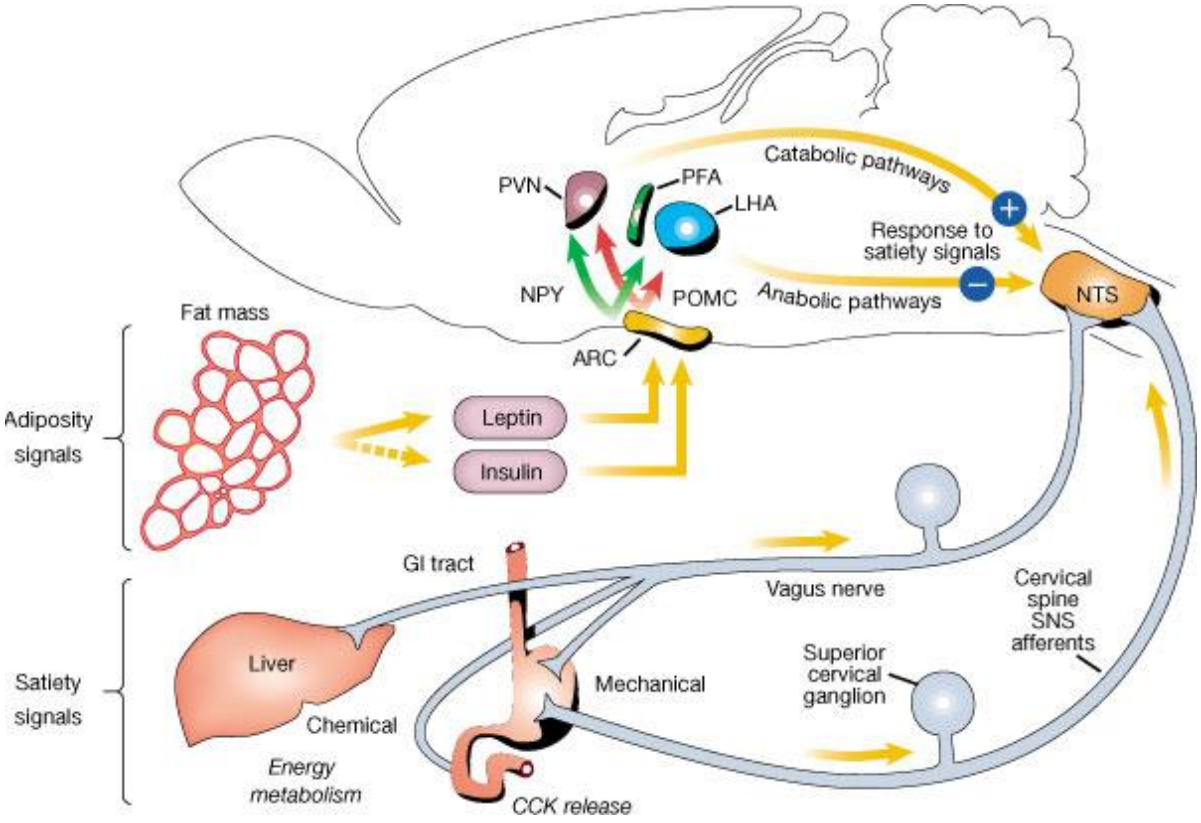

Figure 2: Insulin and leptin signalling controlling energy intake and expenditure in the brain[56]

1.3.3 Inflammation and PTP1B

Studies from the last decade have shown epidemiological, clinical and experimental evidence that obesity and related diseases are associated with chronic, low-grade inflammation in the blood and in peripheral tissues[61]. The link between obesity and inflammation in both the hypothalamus and peripheral tissue has been explained by several mechanisms, including activation of toll-like receptor 4 (TLR4), induction of ER-stress, and activation of serine/threonine kinases, such as IKKβ[62]. Overnutrition-induced neuroinflammation leads to dysfunctions in the CNS in obesity and T2D[61]. Neuroinflammation has negative impacts on neurohormonal signalling of hypothalamic neurons[61], which influences the feeding behaviour. Hypothalamic inflammation induced by HFD leads to neuron injury that triggers reactive gliosis involving both microglia and astrocytes[19]. This neuroinflammation occurs selectively in the arcuate nucleus of the hypothalamus and quickly occurs after the initiation of HFD, in both humans and rodents[19]. The quickly occurring inflammation suggests that its role is the protection of the neurons against further damage, but sustaining of the HFD may turn the acute inflammation into a chronic process. This makes hypothalamic inflammation an interesting target in the battle against obesity and T2D.

Several studies have shown that PTP1B plays an important role in inflammation[63,64]. PTP1B knock down in a macrophage cell line gave a rise in the production of TNF-α, IL-6 and IFN-β after stimulation with TLR ligands[64]. PTP1B also appears to be involved in macrophage development, through regulation of CSF1 signalling[63]. An increase in

sensitivity of PTP1B deficient macrophages and an increased inflammatory phenotype in response to LPS was seen. This indicated that PTP1B may have an anti-inflammatory role in macrophages. These studies, however, were all performed in either macrophage cell lines or global PTP1B knock out models.

Recently, Grant et al. showed that Lysm-PTP1B mice have improved glucose tolerance, improved insulin levels and suppressed inflammatory response to HFD compared to control mice[13]. This was contradictory to the pro-inflammatory phenotype in the global PTP1B knock out models described before. Lysm-PTP1B bone marrow derived macrophages (BMDMs) expressed lower levels of pro-inflammatory cytokines *in vitro*, which was in agreement with the phenotype of the mouse model. A probable cause for the suppression of TNF-α *in vitro* was the simultaneous increase in transcription and secretion of the anti-inflammatory cytokine, IL-10. Elevated levels of phosphorylated signal transducer and activator of transcription 3 (STAT3), known to mediate the IL-10 driven anti-inflammatory response, also supported this. Downstream components of the IL-10 receptor JAK1 and TYK2 lead to activation of STAT3[65], which causes a positive feedback loop. It has been shown that TYK2 is regulated by PTP1B[66], so the lack of PTP1B could be the reason for the higher levels of pSTAT3. In addition, STAT1 phosphorylation was increased in BMDMs lacking PTP1B. Induction with LPS therefore led to higher levels of iNOS and nitrite. *In vivo*, Lysm-PTP1B also showed increased basal and LPS-induced levels of circulating IL10 compared to control animals, negatively correlating with insulin levels. Interleukin 10 has proven a potent sensitizer of insulin signalling by suppressing the deleterious effects of TNFα and IL6 on insulin signalling[67]. This study indicated that PTP1B plays a pro-inflammatory role in macrophages, contrary to previous reports that describe macrophage PTP1B to be anti-inflammatory.

1.3.4 Role for PTP1B in endoplasmic reticulum (ER) stress

It has been known that inflammation is involved in obesity and T2D and inflammatory processes may be the link between obesity and T2D. But recent research indicates that prolonged high fat feeding also induces endoplasmic reticulum (ER) stress, which contributes to the development of insulin resistance and diabetes by triggering JNK activity via inositol-requiring enzyme–1 (IRE-1) and inhibition of insulin receptor signalling[10]. Primary and immortalized PTP1B$^{-/-}$ fibroblasts show a decreased ER-stress response through impaired IRE1 signalling[12]. Recent research shows that PTP1B diminishes diet-induced ER-stress[17]. Pharmacological induction of ER-stress on hepatic cells also gives increased levels of PTP1B[68]. The knocking out of liver PTP1B reduces levels of markers for each of the three ER-stress pathways[68]. This suggests that there might be a positive feedback loop between PTP1B expression and the ER-stress pathway.

The ER is an organelle found in eukaryotic cells, it is responsible for the metabolism of complex metabolites and proteins. Accumulation of unfolded or misfolded proteins in the lumen of the ER causes ER-stress and activates a signalling network called the

unfolded protein response (UPR). The UPR restores the functioning of the cell initially by halting protein translation, degrading misfolded proteins, and activating the signalling pathways that lead to increasing the production of molecular chaperones involved in protein folding[69]. If this is not achieved, the UPR leads the cell into apoptosis. Chronic activation of the UPR has been implicated in several diseases, including T2D[10]. Conditions that can trigger ER-stress are glucose or nutrient deprivation, viral infections, lipids, increased synthesis of secretory proteins, and expression of mutant or misfolded proteins[10]. Several of these conditions occur in obesity. Most interestingly, the demand on the protein synthesis machinery in the cells of many secretory organ systems increases with obesity. Also associated with obesity are mechanical cellular stress, excess lipid accumulation, abnormalities in intracellular energy fluxes, and nutrient availability. The chronic ER-stress could be the mechanism by which obesity leads to insulin resistance and T2D.

The UPR pathway can be divided in three separate pathways (fig. 3): protein-kinase-R (PKR)-like endoplasmic reticulum kinase (PERK), inositol-requiring enzyme 1 (IRE1) and activated transcription factor 6 (ATF6)[70]. PERK activates eukaryotic initiation factor 2α (eIF2α) by phosphorylation. eIF2α reduces protein translation in general, which leads to a decrease in the amount of (misfolded) protein in the ER. However, eIF2α also increases the translation of ATF4 which activates several UPR target genes involved in

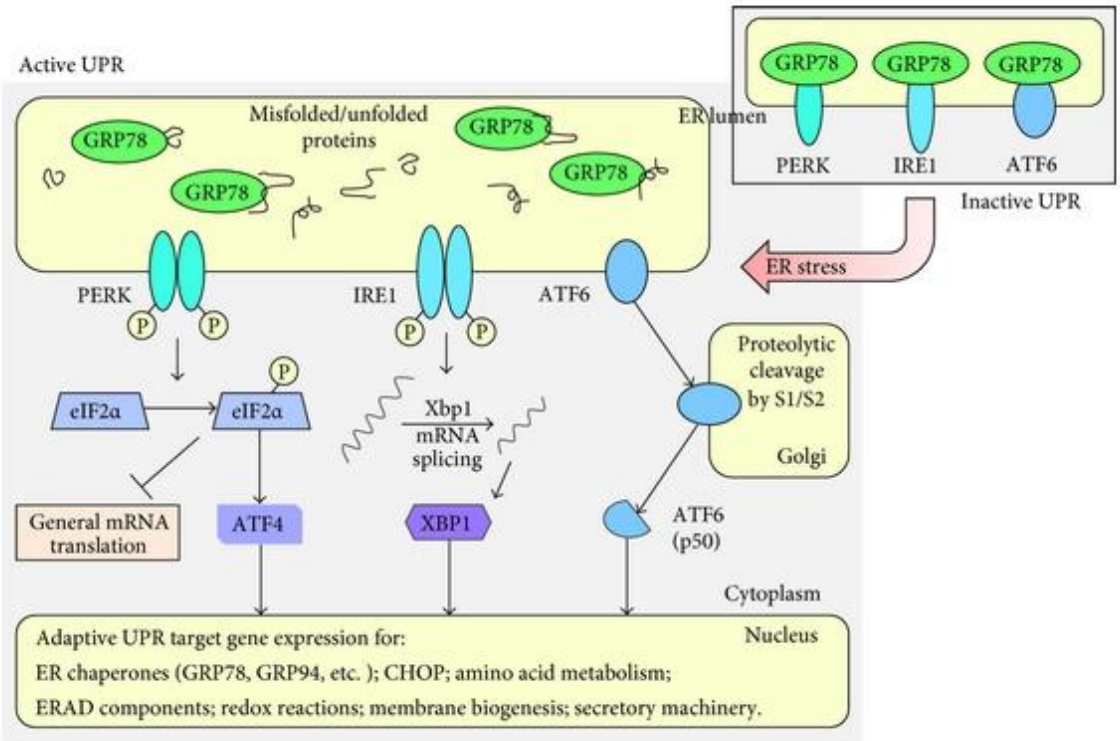

Figure 3: ER-stress pathway[70]

amino acid synthesis and transport, anti-oxidative stress, and apoptosis. One of those genes is CCAAT/enhancer-binding protein homologous protein (CHOP), which induces apoptosis of the cell. IRE1 cleaves XBP1 mRNA which is subsequently translated into the protein XBP1s. XBP1s is a highly reactive transcription factor that regulates the folding of the ER. ATF6 is released by GRP78 and cleaved in the Golgi body. ATF6, together with XBP1s, induces the expression of genes involved in ER-associated degradation. Inhibition of PTP1B seems to be a promising way to reduce ER-stress[17].

1.4 Former research goal

The role of myeloid PTP1B in the periphery is stimulating inflammation, however the effect this model has on inflammation in the brain is not yet known. In the Lysm-PTP1B knock out model all myeloid cells should be PTP1B deficient. This includes bone marrow-derived microglia, which are produced during early embryogenesis. The aim of our study was to determine the *in vitro* inflammatory response of microglia isolated from Lysm-PTP1B (KO) mice in comparison with $PTP1B^{fl/fl}$ (floxed control; WT) mice. The isolation gave only a very low yield (fig. 5) and the deletion of PTP1B could not be confirmed in the isolated cells (fig. 4). Due to these negative results, the aim of the research was changed.

1.5 New research goal

The new objective of this research was to assess the role of myeloid PTP1B in obesity and neuroinflammation. This was examined using Lysm-PTP1B mice on either high fat diet or normal chow diet. Factors of obesity that were examined included: body weight, serum levels of glucose, insulin and leptin and expression of several neuropeptides and receptors involved in energy homeostasis in the hypothalamus. Additionally, expression of inflammatory markers and ER-stress markers in the hypothalamus were investigated. High fat diet has been described previously to increase inflammation in the hypothalamus[19]. Based on the previous results of this model decreasing peripheral inflammation[13], we hypothesized that the lack of PTP1B deletion would also decrease high-fat diet induced neuroinflammation. Chronic inflammation has been linked to ER-stress[10] and liver ER-stress has been shown to decrease in liver-specific PTP1B knock-out mice[68]. Therefore we hypothesized that PTP1B deletion would protect mice form HFD-induced ER-stress.

2. Materials and Methods

2.1 Animals

All animal procedures were performed under a project license approved by the UK Home Office under the Animals (Scientific Procedures) Act 1986. To generate myeloid-PTP1B$^{-/-}$ mice, PTP1B$^{fl/fl}$ mice were crossed with LysM-Cre mice and back-crossed nine times to pure C57BL/6J mice[11]. PTP1B$^{fl/fl}$ mice have LoxP-sites on both sides of the PTP1B locus (floxed), but Cre is absent. Lysm-Cre mice express Cre-recombinase only in myeloid cells. Cre will splice the DNA at the LoxP sites and therefore in the crossed mice PTP1B will be knocked out only in myeloid cells. Lysm-PTP1B mice have PTP1B floxed and Cre expression, so PTP1B will be knocked out in myeloid cells. DNA extraction and genotyping with PCR were performed to check the genotype. Age-matched male and female (ex-breeders) mice were studied and compared to PTP1B$^{fl/fl}$ control littermates. Mice were group-housed and maintained at 22-24°C on 12-hour light/dark cycle with free access to food and water. At either 4 months (young group) or 12 months (old group) the mice were placed on HFD (Adjusted Calories Diet, 55% fat, Harlan Teklad, USA) or continued with standard 3.4% fat chow-pellet diet (Rat and Mouse Breeder and Grower, Special Diets Services, DBM, Scotland) for 15 weeks and weight was recorded weekly. The mice were sacrificed by administration of CO_2 and cervical dislocation, after which tissues (liver, kidney, muscle, white adipose tissue, and brain) and blood were collected. The brain was dissected into hypothalamus, hippocampus and cortex.

2.2 Isolation of microglia cells

Brains were collected immediately after the mice were culled. A mixed glial culture was obtained by a process of mechanical and chemical dissociation of the whole brain excluding the brainstem. The whole brain was minced using two no. 10 scalpels and placed in medium A (Hank's Balanced Salt Solution (HBSS) with 0,585% glucose, 15 mM HEPES, 100 units/ml Penicillin, 100 µg/ml Streptomycin). Minced brain was further dissociated by gentle pipetting. Chemical dissociation was performed by a 20 minute incubation with trypsin medium (Medium A with 0.25% Trypsin, 1000 U/ml DNase I) in a 37°C water bath. Trypsin inhibition medium (Medium A with 20% FCS, 1000 U/ml DNase I, 0.1 mg/ml Trypsin inhibitor) was added to stop the digestion. The pellet was washed with wash medium (Medium A with 10% FCS, 1000 U/ml DNase I). Cells were suspended in DMEM with 10% FCS (DMEM with 10% FCS 1 mM Sodium Pyruvate, 1% L-glutamine, 50 units/ml Penicillin, 50 µg/ml Streptomycin). A single cell suspension was obtained by passing the suspension through a 70 µm cell strainer twice. Cells plated into 75 cm^2 flasks and media were changed every 3 days. On day 10, the mixed glial cultures were shaken by hand 40 times to dislodge microglial cells. The non-adherent cells after shaking were plated onto 6-well or 12-well plates at 1x10^5 cells/ml in 10%FCS-DMEM, and incubated at 37°C. A detailed protocol is provided in appendix C.1.

2.3 Western blotting

Cells were lysed in radio-immunoprecipitation-assay (RIPA) buffer containing fresh sodium-orthovanadate and protease-inhibitors. Protein levels were determined with a BCA assay. Proteins were separated by 4-12% SDS-PAGE and transferred to nitrocellulose membranes. Western blots were performed using antibodies against SHP2 (Santa Cruz), ERK2 (Santa Cruz), β-actin (Sigma) and PTP1B (Millipore). Western blots were visualized using enhanced-chemiluminescence and analysed by using Bio1D software (Peqlab Fusion SL, UK). A detailed protocol is provided in appendix C.2.

2.4 Flow cytometry

Mixed glia cell culture was detached by Accutase (Gibco: A11105-01) and resuspended in 500 µl PBS (Gibco: 14190-094). Cells were plated up (100µl/well) and blocked for 10 minutes in the dark with 1 µl/well rat anti-mouse CD16/CD32 (BD 553141). Cells were labelled with 1µl/well of antibodies: F4/80 AF-700 Rat anti mouse, CD11b PE-CF594 (Texas red) (BD 562287), CD45 PE (BD 553089). As controls non-stained cells, single-stained cells, and plastic beads (positive: BD 51-90-9000949, negative: BD 51-90-9001291) were used. Data were acquired on a flow machine (BD, LSR II) and analysed using FlowJo. A detailed protocol is provided in appendix C.3.

2.5 Gene-expression analysis

Gene expression analysis was done as described before[13]. Tissues were homogenized in Tri-Reagent (Sigma: T924). RNA was extracted using chloroform and isopropanol (Tri-Reagent, Applied Biosystems), a detailed protocol is provided in appendix C.4. RNA levels were determined with a Nanodrop (Jenway Genova Nano). cDNA was synthesized from 1 µg of RNA using Tetro cDNA-synthesis kit (Bioline), following manufacturer's instructions and additional information concerning the protocol is provided in appendix C.5. Quantitive real-time PCR (qPCR) was performed using Light-Cycler 480 (Roche), a detailed protocol is provided in the appendix C.6. Gene expression of iNOS, TNFα, IL6, IL1β, IL1α, IL10, TLR-4, PTP1B, POMC, NPY, CD11b, CD68, LepR, MC4R, Chop, SOCS3, mBACE1vs1, mBACE1vs2, GFAP determined relative to the most stable reference gene (YWhaz, NoNo, HPRT or GAPDH) which was identified using a web-based reference gene assessment tool (http://www.leonxie.com/referencegene.php). Primer sequences are provided in appendix B.

2.6 Blood analysis

Prior to the terminal procedure, tail blood was taken and blood-glucose levels were determined using a glucometer (AlphaTrak, Abbot Logistics). Serum was obtained by post-mortem blood collection. The serum was separated by spinning at 4°C for 10 minutes at 5,000g and stored at -80C. Insulin and leptin levels in the serum were measured with an ELISA (Chrystal Chem. 90080 and 90030, respectively), following manufacturer's instructions. Absorbance was measured at 450nm and 630nm with a plate reader (Versa Max, Molecular Devices).

2.7 Fluorescent cell quantification

Wild-type control mice and Lysm-PTP1B mice received an LPS or saline injection three hours before they were culled. The dentate gyrus of the hypothalamus was stained for DAPI and for GFAP. The relative amount of double positive cells was counted using ImageJ and expressed as a percentage of the amount of DAPI-positive cells.

2.8 Statistical analysis

Data are expressed as mean ± standard deviation. Statistical analyses were performed using two-tailed Student's t-tests and two-way ANOVA's, with Sigmaplot statistical-software. Statistical significance is indicated as follows: (x) p-value < 0.1; (*) p-value < 0.05; (**) p-value < 0.01; and (***) p-value < 0.001 compared to the diet control (chow), and (+) p-value < 0.1; (#) p-value < 0.05; (##) p-value < 0.01; and (###) p-value < 0.001 compared to the genotype control (wild-type).

3. Results

3.1 Effect of myeloid PTP1B knock-out on microglia

Microglia cells were isolated as described in appendix C.1. First, one WT mouse brain was used to test if the protocol worked in our hands. There were too few cells on a large surface of the 75 cm^2 tissue culture flask. After this, microglia from a WT and a Lysm-PTP1B mouse were isolated as a pilot study, to see if there were any differences between the genotypes. They were plated in smaller flasks (25 cm^2) and there were microglia obtained from this, but the yield was too low to detect any protein using Western blot analysis of PTP1B levels. The protocol was changed and microglia from three WT mice and three Lysm-PTP1B mice were isolated. The microglia from the three brains of each genotype were pooled and cultured in one tissue culture dish (25 cm^2). Western blot for PTP1B gave really low protein amounts, and therefore the knock-out of PTP1B in the microglia could not be confirmed with a level of confidence (fig. 4). The Lysm-PTP1B cells were expected to have lower PTP1B levels, but this was not the case. Real-time quantitative PCR was also performed with the microglia, but RNA levels were too low to continue with the protocol. Also, media was collected for cytokine analysis, but this was not analysed since the yield was so low.

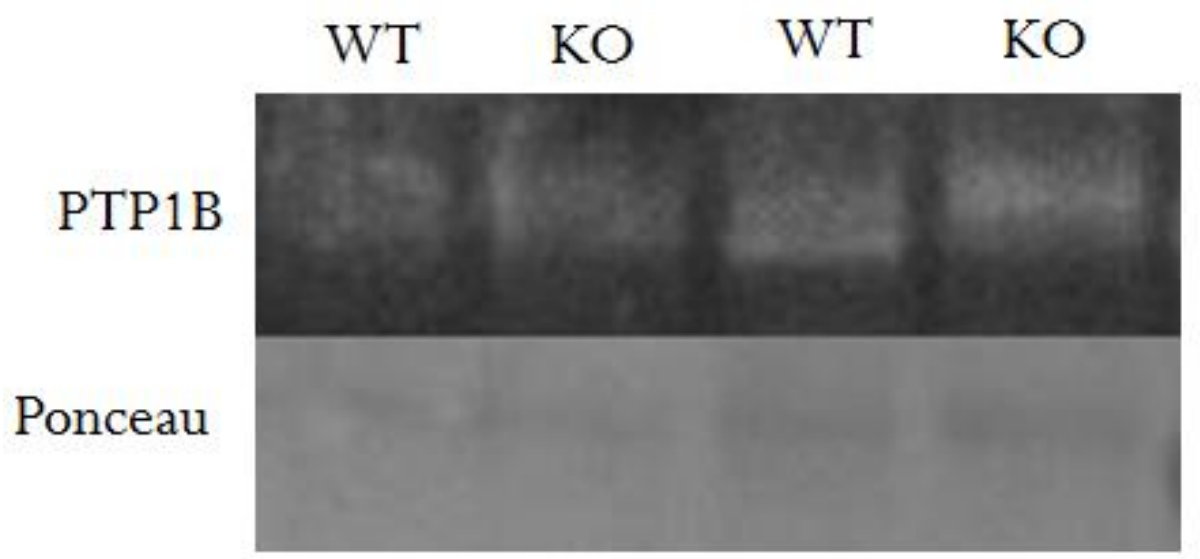

Figure 4: Western blot of PTP1B (top) versus Ponceau control (bottom). Ponceau staining shows the total amount of protein of 55kDa. The PTP1B blot shows the PTP1B protein in microglia of myeloid PTP1B knock-out animals versus WT controls.

Finally, another four WT mice brains were used for microglia isolation in order to confirm the presence and relative amount of microglia in the cell mixture using flow cytometry (fig. 5). The gate in fig. 5a shows the gate that is used to select all live cells, the x-axis represents the forward scattering (FSC) and on the y-axis is the side scattering (SSC). Forward scattering represents the size of the particles and side scattering represents the graininess; double positive cells are presumed to be live cells. Live cells were then plotted for F4/80 and CD11b (fig. 5b), which are markers for microglia and macrophages. The $F4/80^{+}$-$CD11b^{+}$ cell population was selected and plotted in fig. 5c, with F4/80 on the y-axis and CD45 on the x-axis. In microglia CD45 is lowly expressed, so $F4/80^{+}$-$CD11b^{+}$-$CD45^{low}$ are the microglia cells. The ratio of microglia in the live cell population was 5.92%. In fig. 5c/d is the so-called back-gating showed. The selected microglia cells are visible in red in the graphs to show the position of the cells in the whole population. The control graphs show that there are no double positive cells amongst the single stained cells (fig. 6). The graphs show that all single stained controls, CD11b, F4/80 and CD45, are only positive for the antibody they are stained with.

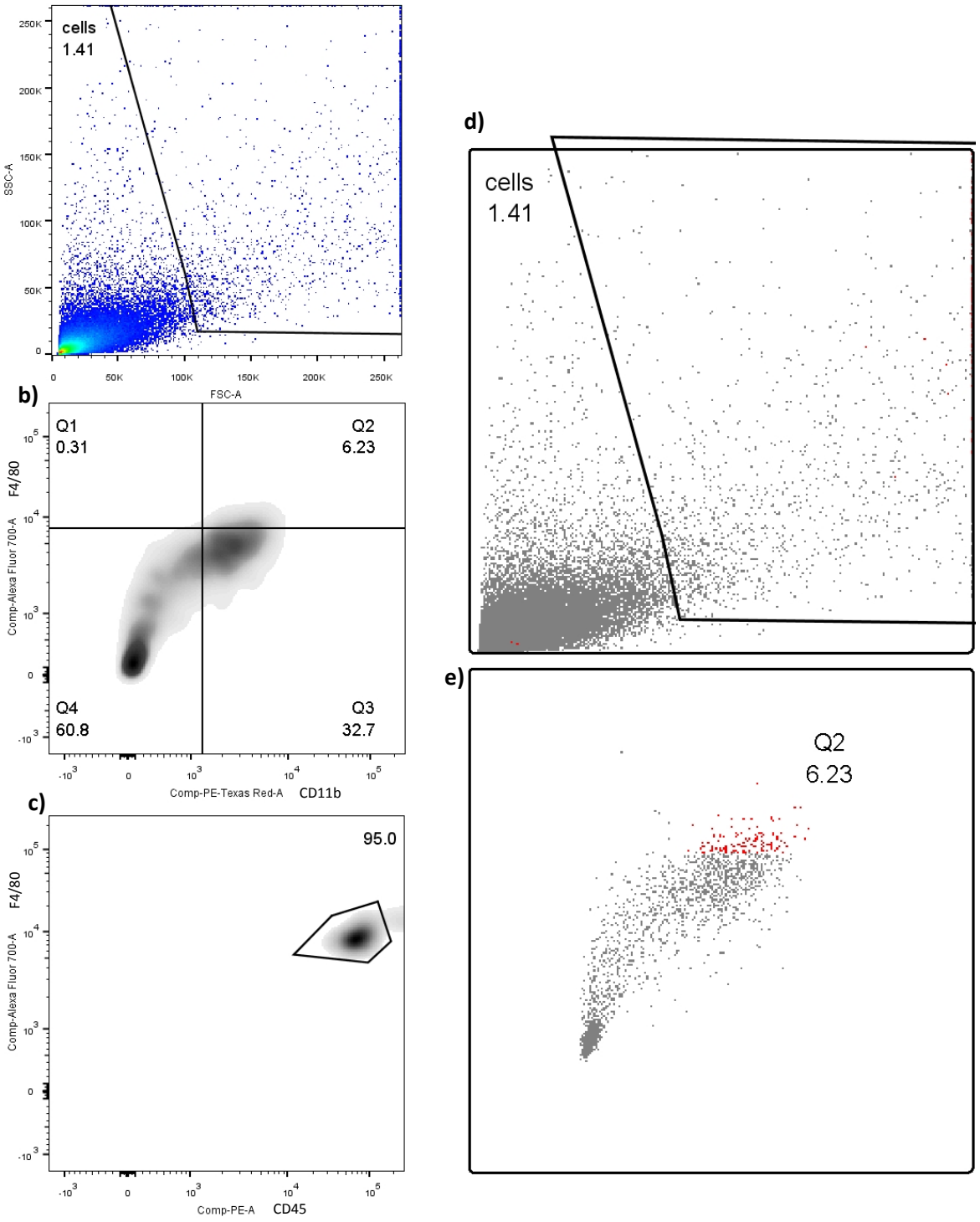

Figure 5: Flow cytometry of microglia of four PTP1B$^{fl/fl}$ control brains pooled (a-e). Live cells are selected based on high side-scatter (SSC) and high forward scatter (FSC) (a). Texas Red is the antibody used for CD11b and Alexa Fluor 700 is the antibody against F4/80. Each line in the graph is the border between the positive and the negative cell population (b). PE is the antibody against CD45 (c). F4/80^{+}-CD11b^{+}-CD45^{low} are the microglia cells (b-c). Back-gating shows the selected microglia in red (d-e).

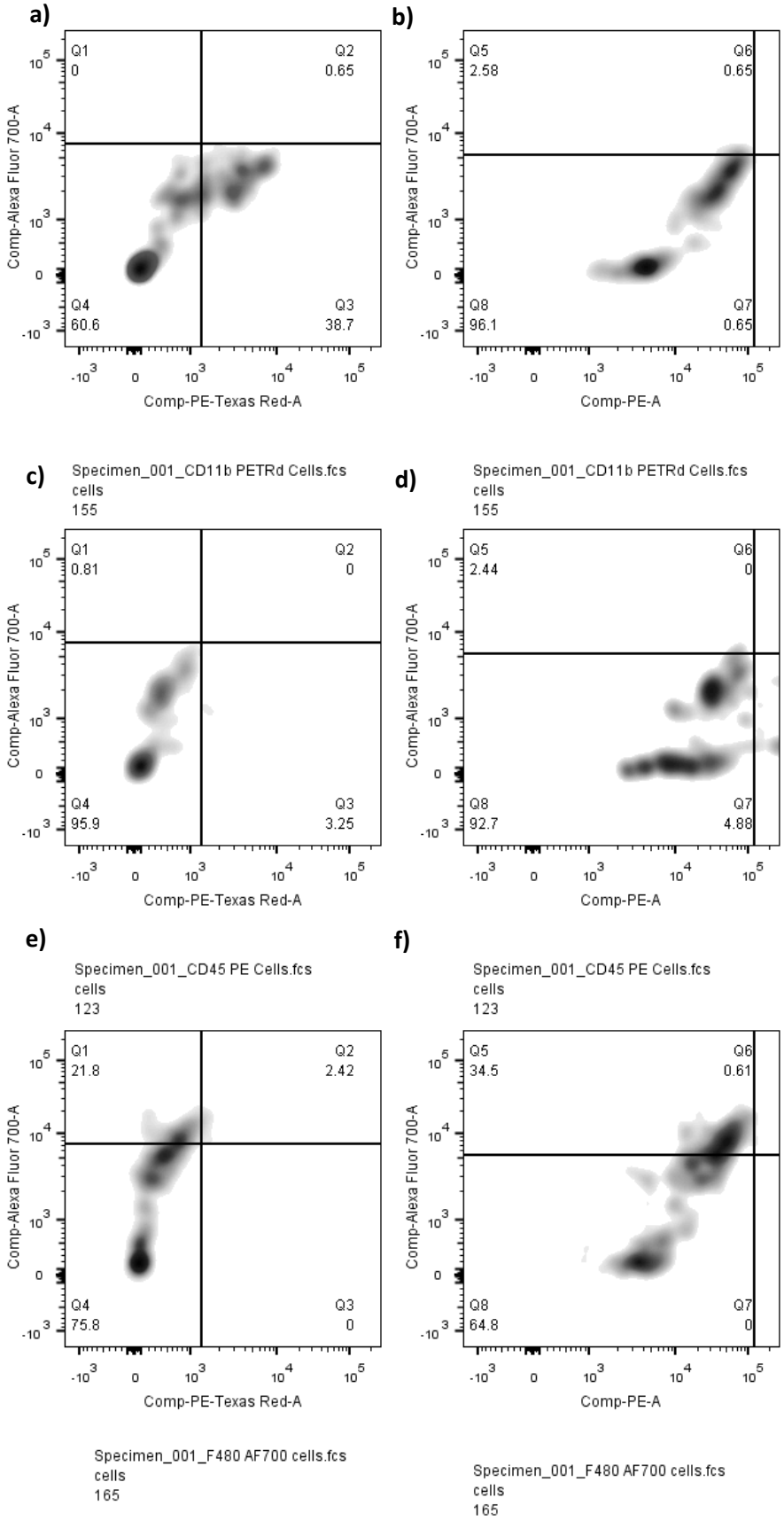

Figure 6: Single stained controls of flow cytometry experiment (a-f). Single stained cells stained with Texas Red for CD11b (a-b). Single stained cells stained with PE for CD45 (b-c). Single stained cells stained with Alexa Fluor 700 for F4/80 (e-f). Each line in the graph is the border between the positive and the negative cell population.

3.2 No effect of myeloid PTP1B on body weight

The mice on HFD experienced a gradual increase in body weight over time, as expected, while the chow-fed animals maintained a constant weight as expected for adult mice (fig. 7). The relative increase in body weight of the HFD mice was significantly higher than the chow controls. There is no difference in weight gain between the two genotypes.

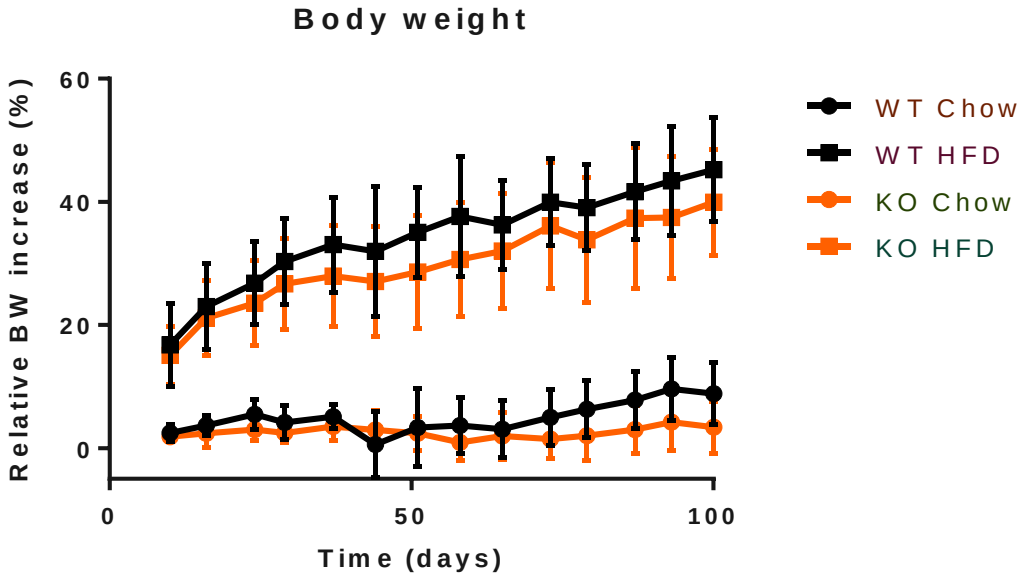

Figure 7: Relative increase in body weight as a percentage of the body weight on day 1 of the diet in Lysm-PTP1B1 mice versus controls under high fat or chow conditions.

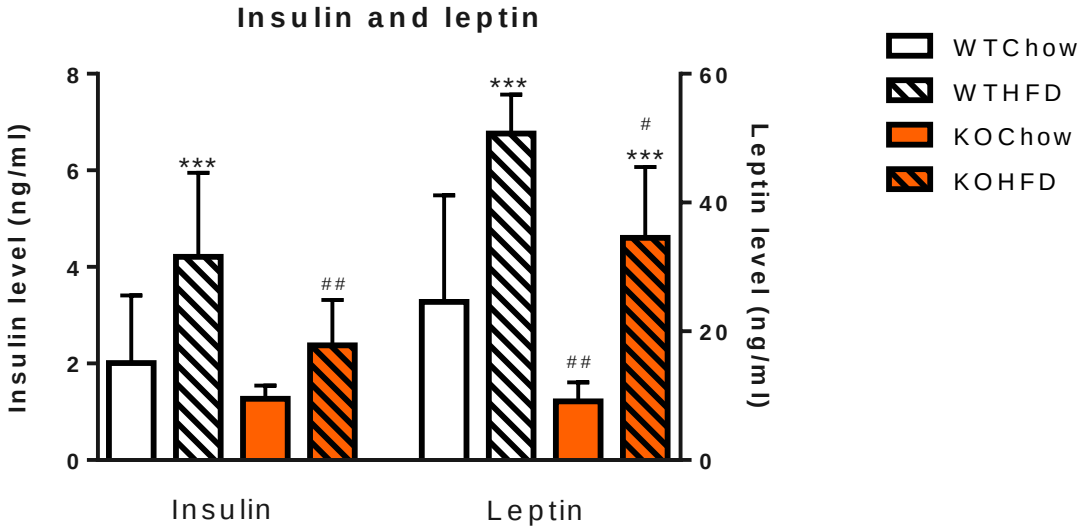

Figure 8: Levels of serum leptin and insulin in Lysm-PTP1B1 mice versus controls under high fat or chow conditions. (x) p-value < 0.1; (*) p-value < 0.05; (**) p-value < 0.01; and (***) p-value < 0.001 compared to the diet control (chow), and (+) p-value < 0.1; (#) p-value < 0.05; (##) p-value < 0.01; and (###) p-value < 0.001 compared to the genotype control (wild-type). Analyses performed using two-tailed Student's t-tests and two-way ANOVA.

3.3 Lysm-PTP1B restores HFD-induced increase in insulin and leptin but not glucose

The insulin levels in the serum of WT mice were increased in the HFD group, whilst in the Lysm-PTP1B these levels were the same level as the chow-fed mice (fig. 8). The absence of myeloid PTP1B did not affect the insulin levels of the chow mice. Circulating leptin levels were also elevated in HFD-fed control WT mice, whilst this was significantly decreased in the Lysm-PTP1B on HFD. Lysm-PTP1B mice on chow diet also had significantly lower leptin levels than the WT mice. On the other hand, blood glucose levels, were unaltered between Lysm-PTP1B and WT mice (fig. 9).

Figure 9: Levels of serum glucose in Lysm-PTP1B1 mice versus controls under high fat or chow conditions. (x) p-value < 0.1; (*) p-value < 0.05; (**) p-value < 0.01; and (***) p-value < 0.001 compared to the diet control (chow), and (+) p-value < 0.1; (#) p-value < 0.05; (##) p-value < 0.01; and (###) p-value < 0.001 compared to the genotype control (wild-type). Analyses performed using two-tailed Student's t-tests and two-way ANOVA.

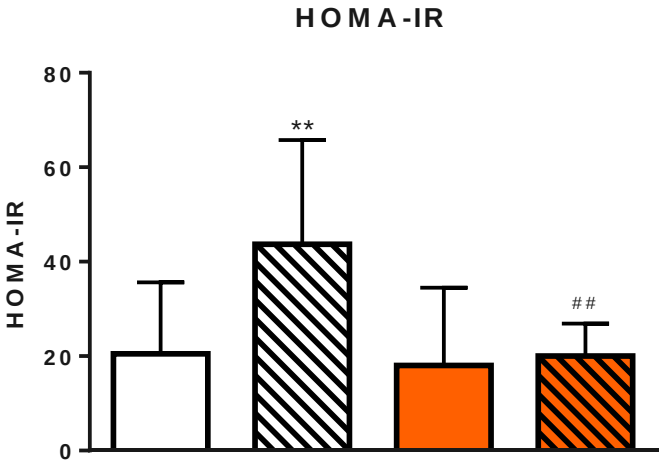

Figure 10: Representation of insulin resistance by the HOMA-IR (Homeostatic model assessment of insulin resistance), calculated by *insulin concentration (μU/ml) * glucose concentration (mM) / 22.5*. (x) p-value < 0.1; (*) p-value < 0.05; (**) p-value < 0.01; and (***) p-value < 0.001 compared to the diet control (chow), and (+) p-value < 0.1; (#) p-value < 0.05; (##) p-value < 0.01; and (###) p-value < 0.001 compared to the genotype control (wild-type). Analyses performed using two-tailed Student's t-tests and two-way ANOVA.

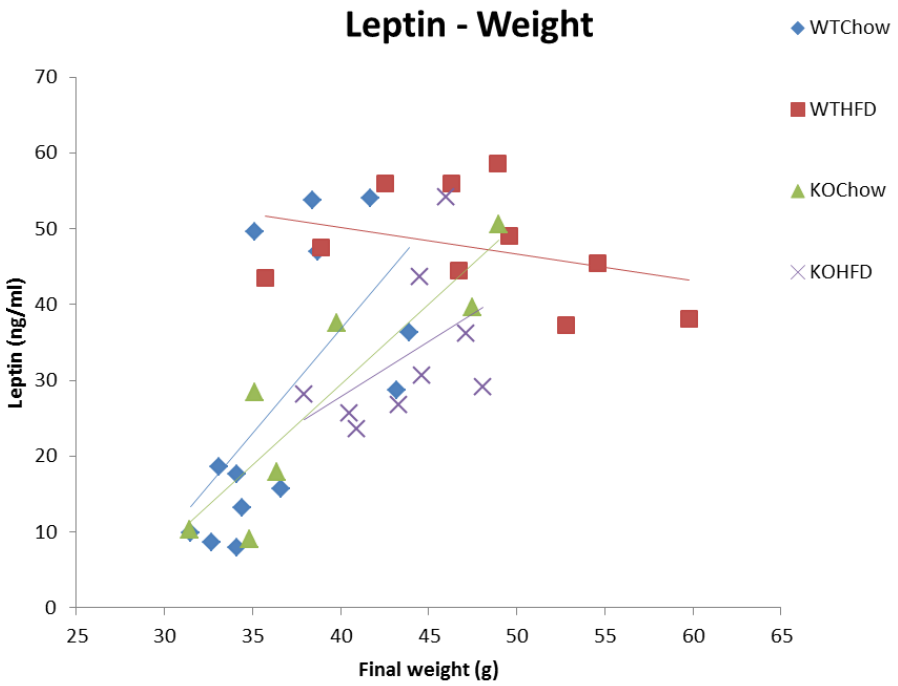

Figure 11: Correlation between the serum leptin levels and the body masses in the different groups (body weights on last week of diet). WTChow: y=2.761x-73.648, R^2=0.3961; WTHFD: y=-0.3503x + 64.266, R^2=0.1196; KOChow: y=2.1163x-55.176, R^2=0.7999; KOHFD: y=1.4531x-30.302, R^2=0.2359.

A method used to determine insulin resistance is the HOMA-IR method[71], calculated by *serum insulin concentration (μU/ml) * serum glucose concentration (mM) / 22.5*. Insulin resistance is significantly up-regulated in HFD-fed mice and the Lysm-PTP1B mice are protected against this (fig. 10). The correlation between serum leptin levels and body weight is shown in fig. 11. In WT chow animals, there is a clear correlation between leptin and body weight. The heavier mice produce more leptin. However in the HFD group, this correlation is not there, animals on HFD produce leptin in a weight-independent manner. Lysm-PTP1B mice, seem to be protected against the leptin insensitivity.

3.4 Determining the most stable hypothalamic housekeeping gene

A housekeeping gene is a gene that is assumed to be expressed at the same relative level in the target tissue of all the experimental groups. Expression of target genes, which are presumed to be different throughout the different groups, can then be compared to the housekeeping genes to provide a relative expression ratio. It is very important that the housekeeping gene is stable in the specific tissue examined. We therefore tested several different commonly used housekeeping genes, including YWHAZ, GAPDH, HPRT and NoNo, because these genes are known to be stable. We used RefFinder (http://www.leonxie.com/referencegene.php), a web-based tool for screening reference genes, to compare and rank the tested candidate reference genes. We

determined that NoNo was the most stable gene in our mice and NoNo was therefore used as housekeeping gene in subsequent experiments (fig. 12).

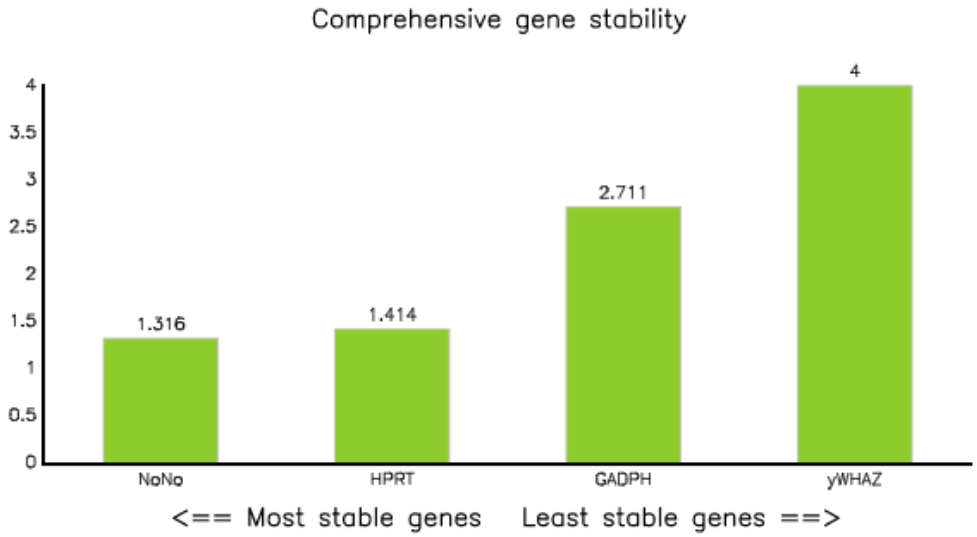

Figure 12: Determination of the most stable reference gene using RefFinder.

3.5 Establishing a protocol for qPCR

To analyse expression levels of different hypothalamic genes, there were two different qPCR protocols being used in the lab. To test the difference in results obtained, the same plate was done twice with the two different protocols. The plate was made up with the genes CD11b and CD68 (fig. 13). The difference between the two protocols was the length of the amplification time; one protocol had an amplification time of 10 seconds and the other one had an amplification time of 60 seconds (see appendix C.6 for the protocol). The longer protocol was on average 1.1 cycles higher for CD11b and 0.7 cycles higher for CD68. This indicates that there is not much difference between the protocols and that the longer protocol even needs more cycles to reach the threshold level.

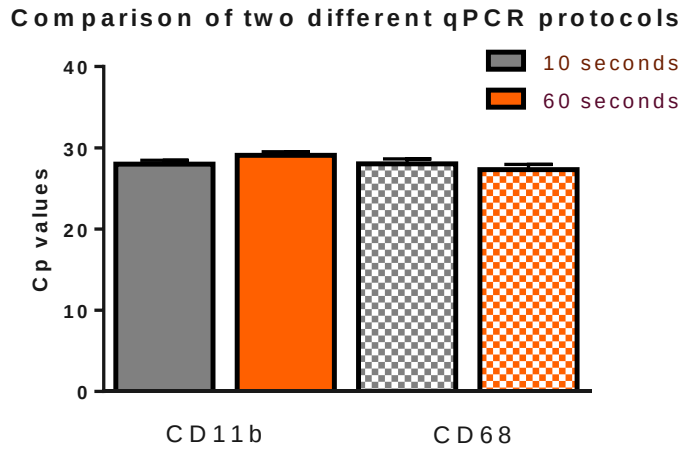

Figure 13: Comparison of the Cp values of two different protocols: one with a short amplification time of 10 seconds and one with a longer amplification time of 60 seconds.

3.6 Levels of PTP1B gene are unaltered in the hypothalamus under HFD conditions

Knocking out myeloid PTP1B could lower the amount of PTP1B-mRNA in the hypothalamus depending on the relative number of myeloid cells present, but there was no effect in the Lysm-PTP1B (fig. 14). Expression of PTP1B was expected to be increased in the hypothalamus under HFD conditions, however this effect was not observed in our HFD mice (fig. 14).

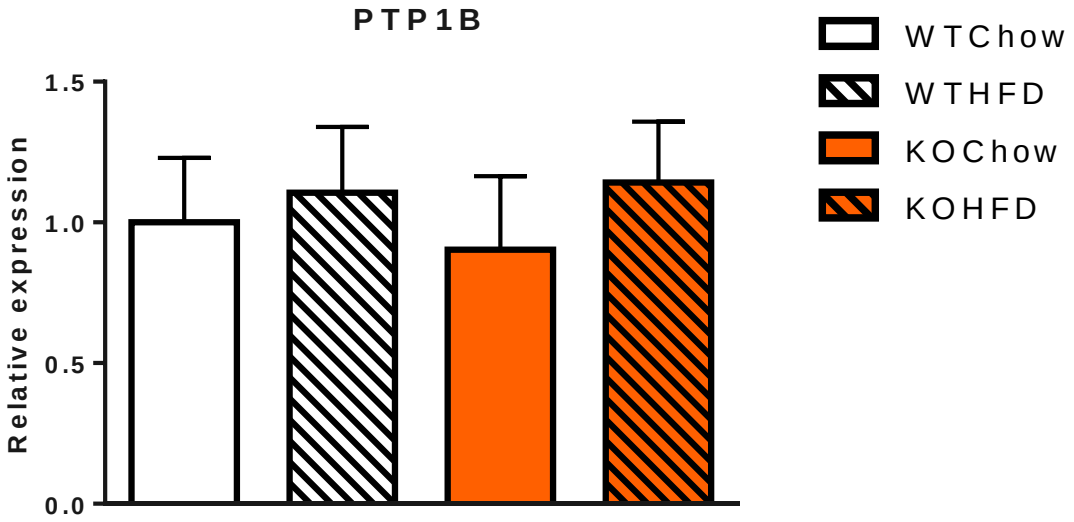

Figure 14: Hypothalamic expression of genes encoding PTP1B in Lysm-PTP1B1 mice versus controls under high fat or chow conditions. (x) p-value < 0.1; (*) p-value < 0.05; (**) p-value < 0.01; and (***) p-value < 0.001 compared to the diet control (chow), and (+) p-value < 0.1; (#) p-value < 0.05; (##) p-value < 0.01; and (###) p-value < 0.001 compared to the genotype control (wild-type). Analyses performed using two-tailed Student's t-tests and two-way ANOVA.

3.7 Influence of myeloid PTP1B on regulators of feeding behaviour

The neuropeptide NPY was down-regulated in the Lysm-PTP1B on chow diet compared to the WT controls (fig. 15). The decrease in NPY was not seen in the HFD-fed mice. HFD did not seem to have an effect on the NPY expression levels in the chow fed animals.

High fat diet did raise the expression of POMC in the hypothalamus (fig. 15). Lysm-PTP1B mouse on chow did have lower POMC levels than the controls, but this decrease was not seen in HFD-fed mice. Insulin receptors (InsR) in the hypothalamus were slightly up-regulated in the Lysm-PTP1B (fig. 16), although this effect disappeared with the HFD. Melanocortin-4 receptors (MC4R) were significantly down-regulated in Lysm-PTP1B (fig. 16). High fat diet increased the MC4R levels back to the same level as the control.

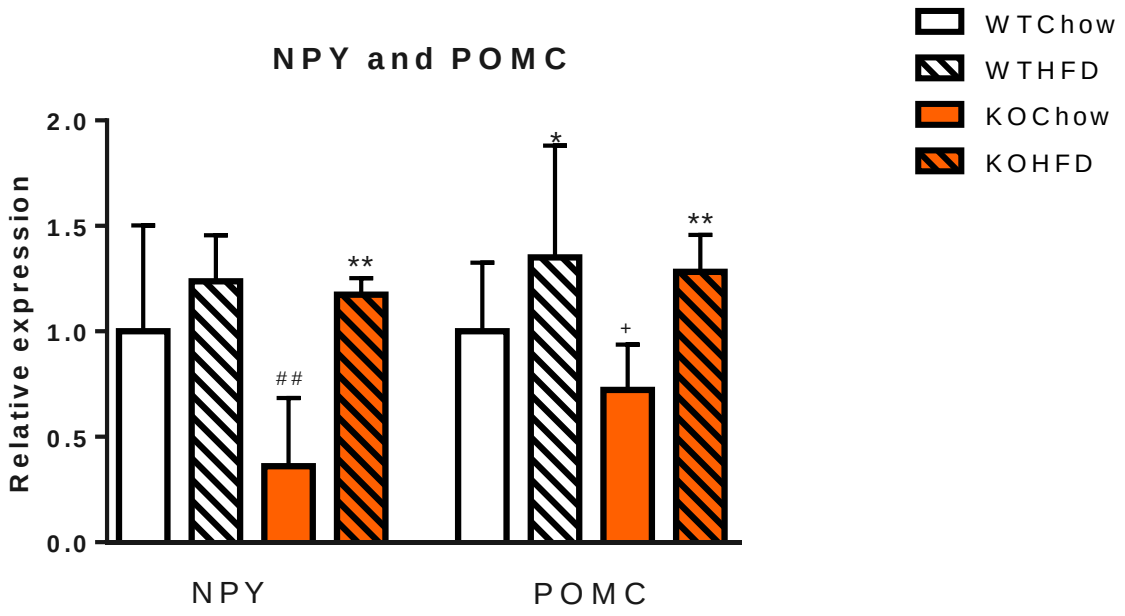

Figure 15: Hypothalamic expression of genes encoding the neuropeptides NPY and POMC in Lysm-PTP1B1 mice versus controls under high fat or chow conditions. (x) p-value < 0.1; (*) p-value < 0.05; (**) p-value < 0.01; and (***) p-value < 0.001 compared to the diet control (chow), and (+) p-value < 0.1; (#) p-value < 0.05; (##) p-value < 0.01; and (###) p-value < 0.001 compared to the genotype control (wild-type). Analyses performed using two-tailed Student's t-tests and two-way ANOVA.

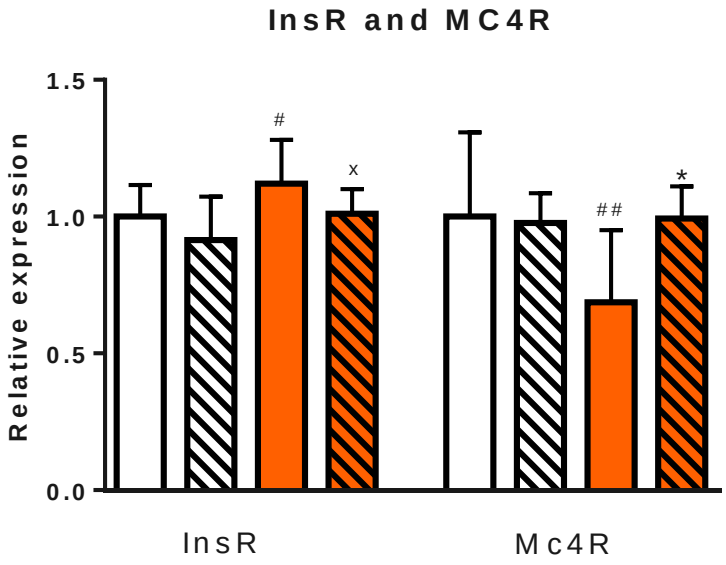

Figure 16: Hypothalamic expression of genes encoding the insulin and MC4 receptor in Lysm-PTP1B1 mice versus controls under high fat or chow conditions. (x) p-value < 0.1; (*) p-value < 0.05; (**) p-value < 0.01; and (***) p-value < 0.001 compared to the diet control (chow), and (+) p-value < 0.1; (#) p-value < 0.05; (##) p-value < 0.01; and (###) p-value < 0.001 compared to the genotype control (wild-type). Analyses performed using two-tailed Student's t-tests and two-way ANOVA.

3.8 Effects of myeloid PTP1B on hypothalamic inflammation

There was a trend towards an increase in TNF-α expression in the hypothalami of Lysm-PTP1B, which was enhanced by HFD (fig. 17). However these results were quite variable, so there were no significant differences. Also, the Cp-values of TNF-α were between 35 and 40 cycles, which makes the results less reliable. The expression of other inflammatory mediators, including IL-1β, IL-6, iNOS, SOCS3 and IL-10, was not detectable. The controls without reverse transcriptase showed the same Cp-values as the samples, thus indicating that this was just background noise. This can have happened because of so-called primer dimers; polymerase replicates the primer dimer instead of the actual DNA. A reasonable explanation for this event is a very low expression of the inflammatory genes in the hypothalamus.

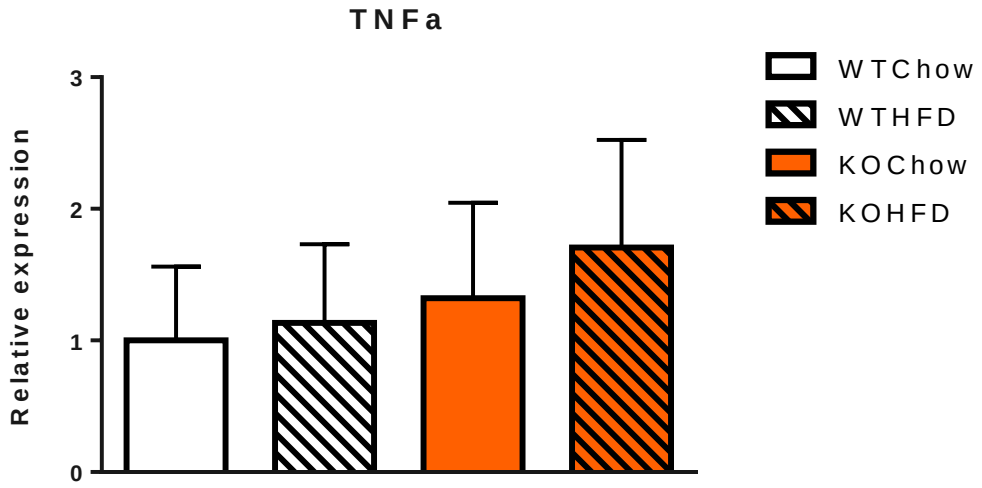

Figure 17: Hypothalamic expression of genes encoding TNF-α in Lysm-PTP1B1 mice versus controls under high fat or chow conditions. (x) p-value < 0.1; (*) p-value < 0.05; (**) p-value < 0.01; and (***) p-value < 0.001 compared to the diet control (chow), and (+) p-value < 0.1; (#) p-value < 0.05; (##) p-value < 0.01; and (###) p-value < 0.001 compared to the genotype control (wild-type). Analyses performed using two-tailed Student's t-tests and two-way ANOVA.

3.9 Microglial activation markers are increased in Lysm-PTP1B on HFD

To measure the activation of microglia, two microglial activation markers were used: CD11b and CD68. CD11b and CD68 are commonly expressed on microglia[72], so they can be used as markers activated microglia. The microglial markers were both up-regulated in the Lysm-PTP1B mice on HFD, but not by HFD feeding alone in WT mice or Lysm-PTP1B chow-fed mice (fig. 18).

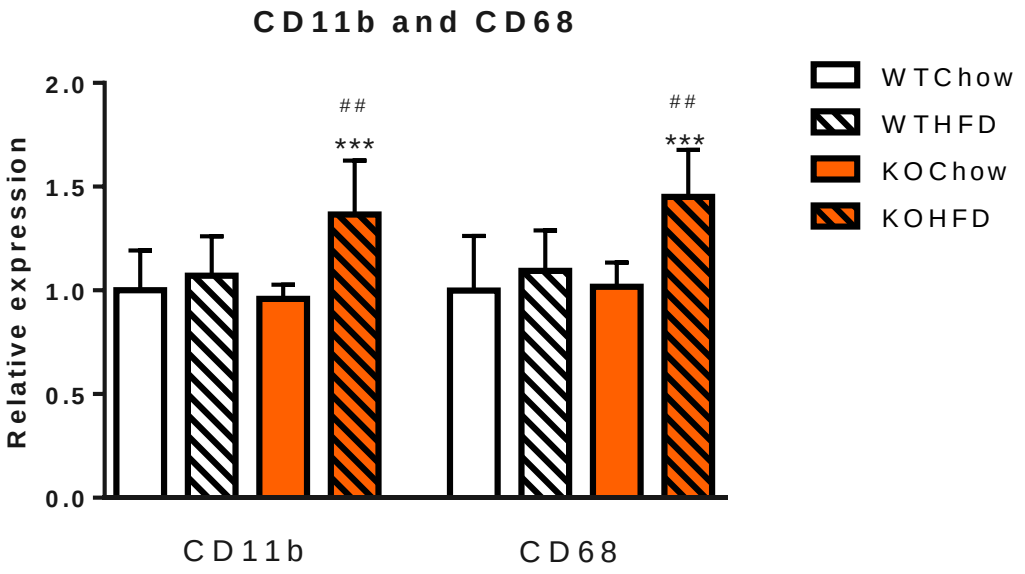

Figure 18: Hypothalamic expression of genes encoding microglia activation markers in Lysm-PTP1B1 mice versus controls under high fat or chow conditions. (x) p-value < 0.1; (*) p-value < 0.05; (**) p-value < 0.01; and (***) p-value < 0.001 compared to the diet control (chow), and (+) p-value < 0.1; (#) p-value < 0.05; (##) p-value < 0.01; and (###) p-value < 0.001 compared to the genotype control (wild-type). Analyses performed using two-tailed Student's t-tests and two-way ANOVA.

3.10 Effect of myeloid PTP1B on HFD- and LPS-induced inflammation in astrocytes

Hypothalamic GFAP is unaltered in HFD as well as in the Lysm-PTP1B mice (fig. 19). The protein GFAP is an intermediate filament that is mainly expressed in astrocytes and therefore acts as a marker for astrogliosis in the hypothalamus. No increase in hypothalamic GFAP was found. This correlates with the results from hypothalamus staining for GFAP. WT control mice and Lysm-PTP1B mice received an LPS or saline injection 3 hours before they were culled. The dentate gyrus of the hippocampus was stained for DAPI and for GFAP. The relative amount of double positive cells was counted and expressed as a percentage of the amount of DAPI-positive cells. No differences were found between the different groups (fig. 20).

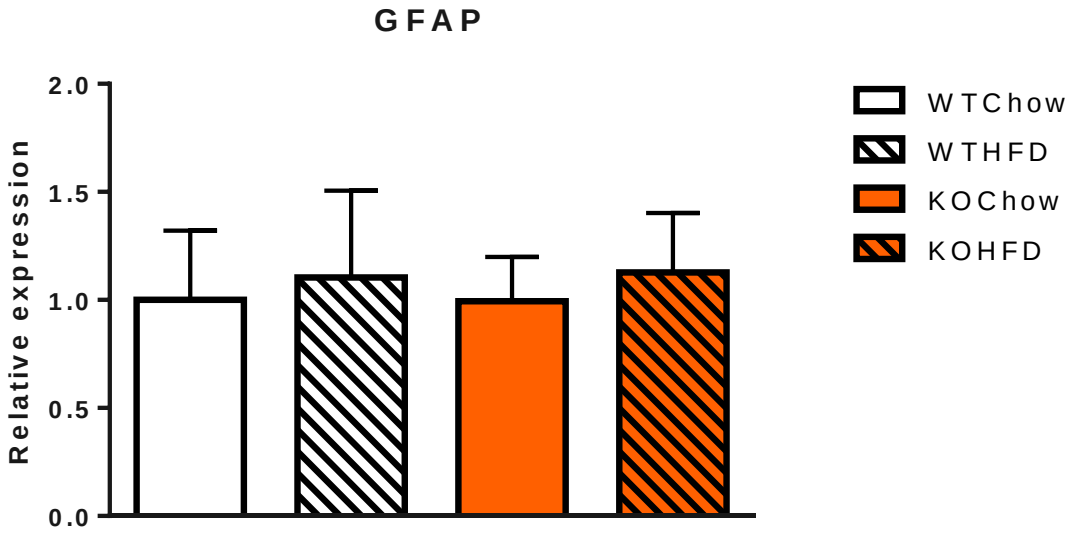

Figure 19: Hypothalamic expression of genes encoding GFAP in Lysm-PTP1B1 mice versus controls under high fat or chow conditions (a). Number of GFAP⁺ stained cells in the dentate gyrus of the hypothalamus relative to the number of DAPI⁺ cells (b). (x) p-value < 0.1; (*) p-value < 0.05; (**) p-value < 0.01; and (***) p-value < 0.001 compared to the diet control (chow), and (+) p-value < 0.1; (#) p-value < 0.05; (##) p-value < 0.01; and (###) p-value < 0.001 compared to the genotype control (wild-type). Analyses performed using two-tailed Student's t-tests and two-way ANOVA.

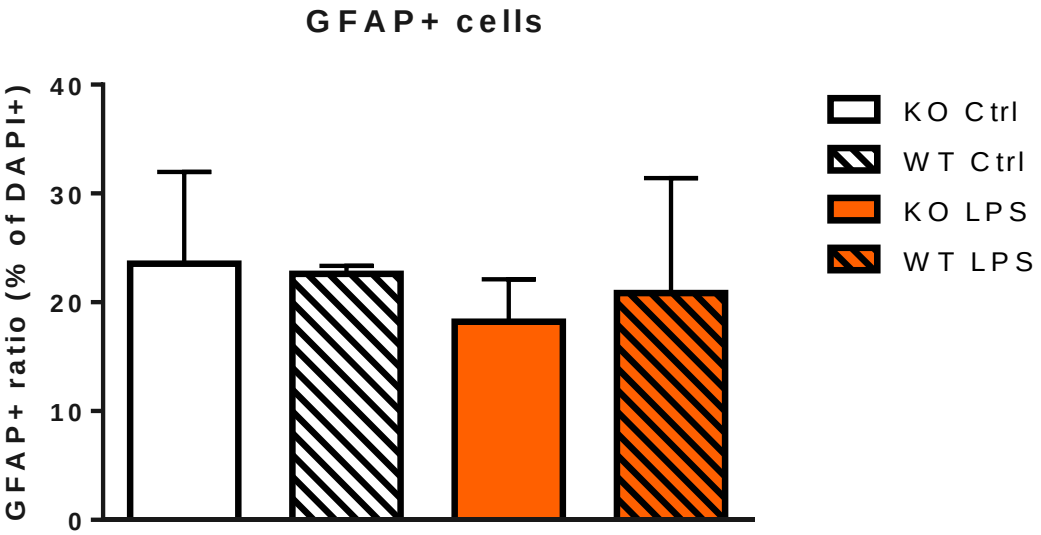

Figure 20: Hypothalamic expression of genes encoding GFAP in Lysm-PTP1B1 mice versus controls under high fat or chow conditions (a). Number of GFAP⁺ stained cells in the dentate gyrus of the hypothalamus relative to the number of DAPI⁺ cells (b). (x) p-value < 0.1; (*) p-value < 0.05; (**) p-value < 0.01; and (***) p-value < 0.001 compared to the diet control (chow), and (+) p-value < 0.1; (#) p-value < 0.05; (##) p-value < 0.01; and (###) p-value < 0.001 compared to the genotype control (wild-type). Analyses performed using two-tailed Student's t-tests and two-way ANOVA.

3.11 Gene expression of ER-stress markers is decreased in Lysm-PTP1B mice

The effect of myeloid PTP1B on HFD-induced hypothalamic ER-stress was analysed by measuring mRNA levels of several genes involved in two different pathways of UPR-signalling (fig. 3). Both ATF4 and CHOP were slightly up-regulated in HFD-fed WT mice, but the knock-out of myeloid PTP1B could not rescue that phenotype (fig. 21). The transcription factor XBP1 was unaffected in HFD, while the spliced version of XBP1 (XBP1s) was up-regulated in HFD (fig. 22). This suggests that XBP1 was up-regulated and splicing was increased. Interestingly, both XBP1 and XBP1s were significantly lower in the Lysm-PTP1B. However this effect was only seen in chow-fed animals, whilst the Lysm-PTP1B mice on HFD had no decrease in levels of XBP1 or XBP1s compared to the WT controls.

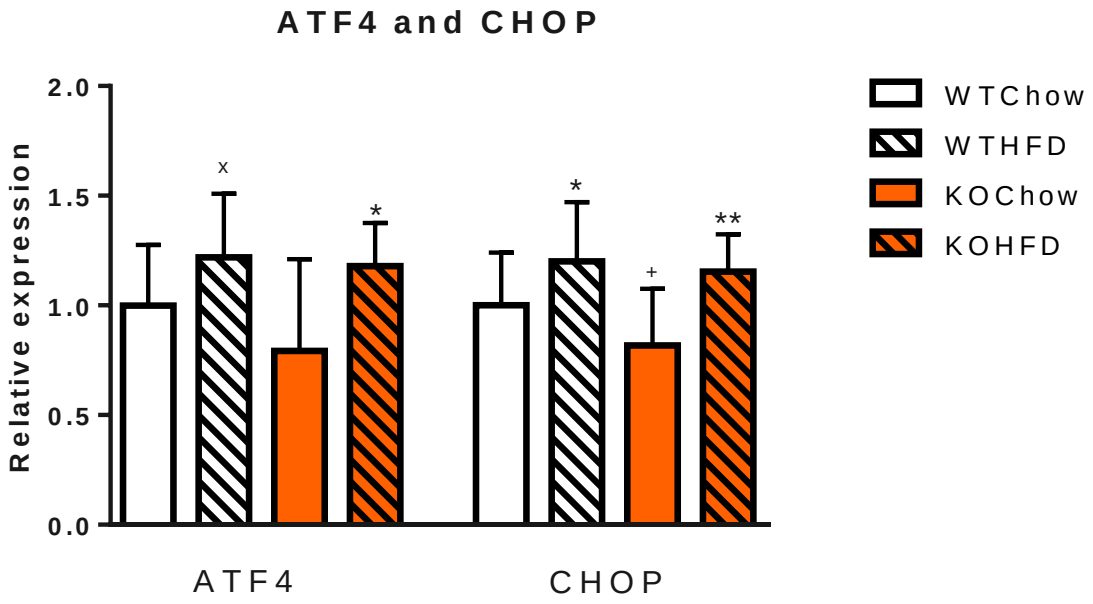

Figure 21: Hypothalamic expression of genes encoding ER-stress markers of the PERK (a) and the IRE1 (b) pathway in Lysm-PTP1B1 mice versus controls under high fat or chow conditions. (x) p-value < 0.1; (*) p-value < 0.05; (**) p-value < 0.01; and (***) p-value < 0.001 compared to the diet control (chow), and (+) p-value < 0.1; (#) p-value < 0.05; (##) p-value < 0.01; and (###) p-value < 0.001 compared to the genotype control (wild-type). Analyses performed using two-tailed Student's t-tests and two-way ANOVA.

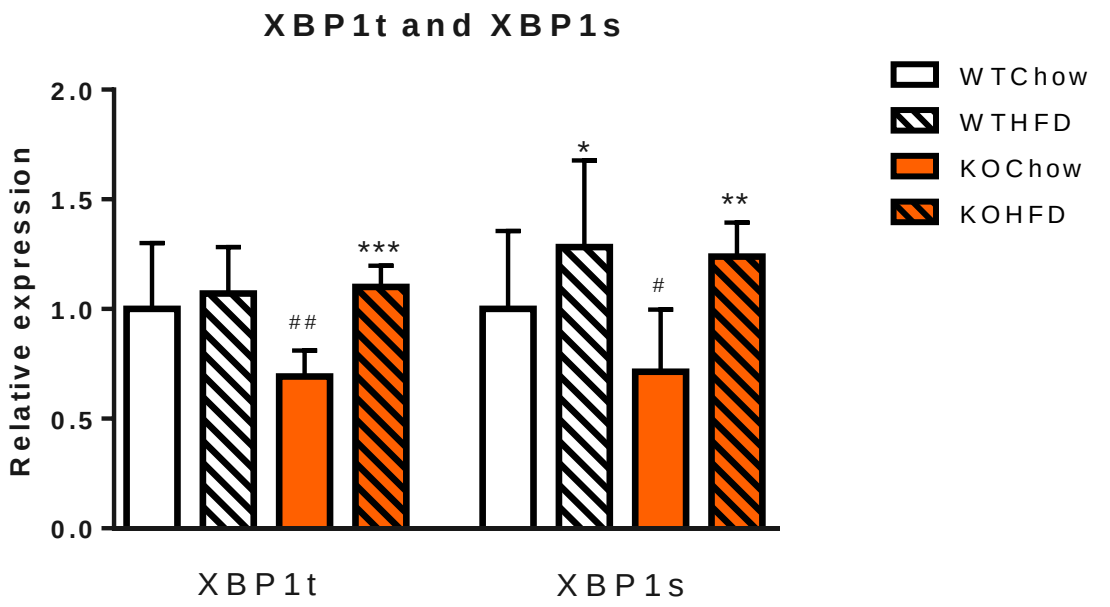

Figure 22: Hypothalamic expression of genes encoding ER-stress markers of the PERK (a) and the IRE1 (b) pathway in Lysm-PTP1B1 mice versus controls under high fat or chow conditions. (x) p-value < 0.1; (*) p-value < 0.05; (**) p-value < 0.01; and (***) p-value < 0.001 compared to the diet control (chow), and (+) p-value < 0.1; (#) p-value < 0.05; (##) p-value < 0.01; and (###) p-value < 0.001 compared to the genotype control (wild-type). Analyses performed using two-tailed Student's t-tests and two-way ANOVA.

4. Discussion

Obesity is an escalating problem that poses a major threat to human health worldwide[3]. The increase in obesity in the near future is even more alarming[4]. Interventions are needed, but effective therapies to cure or prevent the development of obesity are limited. In this study, the goal was to find how PTP1B deletion in immune cells, i.e. microglia, would affect insulin and leptin signalling, inflammation and ER-stress in the hypothalamus. We found that the deletion of myeloid PTP1B does not affect the increase in body weight in HFD fed mice (fig. 7). However, the Lysm-PTP1B mice are protected against HFD induced insulin resistance as well as leptin resistance (fig. 8, 10-11). The results regarding the effect of HFD and PTP1B deletion on hypothalamic insulin and leptin resistance are not conclusive (fig. 15-16). Microglia/macrophage markers CD11b and CD68 are up-regulated in the Lysm-PTP1B mice on HFD (fig. 18), indicating infiltration of microglia or brain-residing macrophages into the hypothalamus of these mice. There is a slight up-regulation in the control mice on HFD as well, but this is not significant. These results suggest that there is a minor increase in hypothalamic inflammation under high-fat conditions, and this effect is boosted by the deletion of PTP1B. Tumour necrosis factor-α was unchanged (fig. 17) and several other inflammatory markers were not detectable in the hypothalamus. There was no increase in GFAP in the hypothalamus, although it was again slightly up in the HFD mice, indicating that there was no infiltration of astrocytes (fig. 19). Lysm-PTP1B mice are protected against ER-stress via the XBP-1 pathway, but this effect was not persistent in mice on HFD (fig. 22). In summary, the effects of myeloid PTP1B deletion protects against HFD induced insulin and leptin resistance, but do not affect inflammation or ER-stress levels.

4.1 Microglia isolation

To investigate the effects of myeloid PTP1B on neuroinflammation, microglia cells were isolated from mature mice. Differences in inflammatory response after LPS stimulation, were to be measured with qPCR. However, microglia cells were not obtained in high enough numbers in order to examine protein or RNA levels. This negative result could be due to the isolation procedure. Normally, isolation of microglial cells is normally performed on pups right after birth or within a few days. Isolation of microglial cells from mature mice has been done before, however in most cases other protocols were used with more complex techniques[73,74]. The plan was to obtain the cells from mature animals in order to also include the effect of diet. Small sets of young pups with different genotypes could have been used in order to get a microglia culture going. In that way tests could have been done on microglia directly, although diet would not have been included. There was no time anymore to do so, but this can be done in future studies. Also, an LPS injection before culling the animals could have potentially increased the microglia yield[74]. However, this could also interfere with the behaviour of the microglia in vitro, because microglia isolated from mice injected with LPS have a more proinflammatory phenotype[74].

Another issue concerning microglia isolation from the Lysm-PTP1B mice is the origin of microglia. The hypothesis of microglia lacking PTP1B was based on the assumption that brain microglia originate from myeloid cells in the bone marrow. However, probably only a small portion of the brain's microglia cells are actually bone-marrow derived, the majority of microglia originates from the yolk-sac[72]. This could be an explanation for the lack of PTP1B deletion in the Western blot analysis of the microglia cells (fig. 4). If the isolated microglia are mostly yolk-sac derived, most of them will still express PTP1B, because it is only knocked out in myeloid cells. The overall live microglia yield was very low (fig. 5), otherwise the myeloid-derived microglia could have been separated from the yolk-sac-derived microglia after isolation by fluorescence-activated cell sorting (FACS). The new objective of this research was to assess the role of myeloid PTP1B in obesity and neuroinflammation. Factors of obesity that were examined included: body weight, serum levels of glucose, insulin and leptin and expression of several neuropeptides and receptors involved in energy homeostasis in the hypothalamus. Additionally, expression of inflammatory markers and ER-stress markers in the hypothalamus were investigated.

4.2 *No effect of myeloid PTP1B on body weight*

The PTP1B knock-out did not slow down the weight gain of the mice on HFD (fig. 7). Although on several time points, the weight gain of the knock-out mice is slightly lower than the control mice, it is not nearly comparable to the mice on chow diet. A problem could be that the fat content in the diet was too high in order for Lysm-PTP1B to have any effect or the time period of the diet could have been too short to have an effect. This in in agreement with Grant et al., who also found there were no differences in body weight between WT and LysM-PTP1B mice on chow or HFD and HFD equivalently increased the body weight in both groups.

4.3 Effect of myeloid PTP1B on circulating levels of insulin, leptin and glucose

The decrease of plasma insulin levels in the knock-out group on HFD compared to the WT on HFD (fig. 8) indicates that the lack of myeloid PTP1B leads to a less desensitized insulin signalling, meaning that insulin signalling under HFD conditions is improved by interfering with myeloid PTP1B. Obesity and HFD lead to insulin resistance and therefore increased insulin levels[75], which is confirmed by our results. The raised insulin levels in the high fat diet group mean that the insulin signalling has been blunted and the body tries to compensate by producing more insulin. Furthermore, the insulin resistance as determined by the HOMA (fig. 10) shows that the Lysm-PTP1B mice are protected against the increased insulin resistance under HFD conditions. In addition, the insulin levels of chow mice are not affected by the KO-model (fig. 8). This show that the inhibition of myeloid PTP1B restores the insulin levels back to levels comparable with mice on normal diet.

The leptin levels of mice on HFD (fig. 8) in the Lysm-PTP1B are lower than the WT mice. So besides the sensitizing of the insulin signalling, also the leptin pathway is sensitized. Leptin levels in the blood correlate positively with adipose mass, indicating the occurrence of leptin resistance, and obese individuals have high levels of leptin without the expected anorexic responses[76]. Mice on chow diet seem to have higher leptin levels if the body mass is higher (fig. 8). However, with mice on HFD this effect seems to be weakened; leptin levels stay similar in mice with varying body masses. Interestingly, the correlation in the Lysm-PTP1B group on HFD is similar to the correlation of the WT animals on chow diet. This could be due to coincidence because there was no significant difference, but it is something to keep in mind in later research.

Plasma glucose levels (fig. 9) are not different in the Lysm-PTP1B mice compared to the WT mice. The fact that there is no rise in glucose in the WT mice on HFD compared to the chow diet, argues for a flaw in the experimental procedure. Normally, it is expected that a long-term HFD gives mice a rise in plasma glucose[75]. The IR from the HFD should impair the suppression of hepatic glucose production and thus gluconeogenesis and glycogenolysis continue at high levels despite normal or high circulating glucose levels.

In summary, the higher levels of both insulin and leptin indicate that the HFD desensitized the insulin and leptin signalling, which was expected. In the KOHFD group, the levels of both insulin and leptin are decreased, indicating that blocking PTP1B in myeloid cells could be a good method of restoring the disturbed insulin and leptin signalling in T2D. It is, however, a result that is not found in previous research with the same model[13]. In the research by Grant et al., no significant differences in leptin and insulin were found between the groups. Previous research has indicated that high-fat feeding affects insulin and leptin signalling[6], which is also the case in our results. And in our study, the insulin and leptin signalling seems to be restored due to the mutation of Lysm-PTP1B.

4.4 Role of myeloid PTP1B in insulin and leptin signalling in the hypothalamus

To establish the role that myeloid PTP1B has in the feeding behaviour, the InsRs and LepRs in the brain needed to be investigated. However, the LR was not measurable, so only the insulin receptor gave results (fig. 16). There were no differences in the expression of the IR in the hypothalamus between the chow fed and HFD fed wild-type mice. The KOChow mice have an upregulated expression of the IR, which could mean that the lack of PTP1B caused a decreased inhibition on the IR. This effect is not seen in the KOHFD group. The upregulated levels of insulin in WTHFD mice indicate that there is insulin resistance. The fact that the InsR is not upregulated due to the HFD could mean that insulin resistance does not occur in the hypothalamus, but only at a peripheral level. However, IR could still happen in the hypothalamus, if downstream signalling agents, such as the IRS, are downregulated.

The HFD does not seem to affect the expression of NPY in WT mice (fig. 15). The KOChow mice have significantly lower NPY expression than the WTChow mice, but the KOHFD mice have a higher NPY again. It seems like the lack of PTP1B affects the NPY expression, but not in combination with HFD. NPY and its receptors act in the response to absent (and possibly low) leptin, whereas αMSH and its receptor, the MC4R are required for the response to an increased plasma leptin concentration[76]. When administered intrathecally, NPY is the most potent orexigenic agent[76]. Although, these findings need to be carefully interpreted, because injecting an agent into the CSF is not really comparable to the natural situation. NPY RNA is increased in ob/ob mice and decreases after leptin treatment, while an NPY-knockout attenuates the obesity and other features of ob/ob mice[77]. Our findings, that NPY is unaltered in WTHFD, while the leptin levels are elevated, are not in line with these previous studies. However, these studies are already quite old and they are based on an ob/ob mouse model. Also, if leptin resistance takes place, than the leptin signalling is disturbed and it is logical that the NPY levels are not affected.

The expression of POMC in the hypothalamus is elevated in HFD (fig. 15). This is not expected, because POMC is expected to be downregulated in response to HFD. Abnormal POMC signalling by disruption of the MC4R results in obesity and LR in mice[78]. High-fat feeding induces IR and LR, which is suggested in our model by raised insulin and leptin levels (fig. 8), and POMC is expected to be downregulated because of less stimulation coming from leptin and insulin. Higher insulin and leptin levels, in response to food intake, normally lead to an increase in POMC and a decrease in NPY, which is good because the food intake will go down and the energy expenditure will go up. However, chronic overfeeding can lead to insulin and leptin resistance. This means that although leptin and insulin levels are high, the signal is decreasing and therefore POMC will be downregulated and NPY upregulated. This leads to an increase in food intake and a decrease in energy expenditure, while being overfed already.

The level of POMC is lower in the KOChow compared to the WTChow and higher again in the KOHFD. The POMC expression seems to be upregulated in HFD condition independent of the genotype. The fact that both the POMC and the NPY in KOChow are lower than in WTChow indicates that myeloid PTP1B mutation somehow influences the expression of NPY and POMC, that could be caused by the disruption of the inhibiting signal of PTP1B on insulin and leptin signalling. Mice lacking PTP1B specifically in POMC neurons display reduced adiposity, improved leptin sensitivity, increased energy expenditure and improved glucose homeostasis on HFD compared with WT mice[79]. This indicates that PTP1B does have an effect on POMC in the hypothalamus, but apparently not through myeloid cells. The MC4R, where α-MSH from POMC neurons binds to, was not affected by HFD (fig 16). Only in KOChow animals the MC4R is downregulated, which is in line with the observed decrease in POMC.

4.5 Inflammation and PTP1B

Inflammation is an important mechanism associated with obesity, IR and T2D. Insulin resistance is aggravated in muscle, liver and adipose tissue in obesity, because of chronic, low-grade inflammation and macrophage infiltration in these tissues[80]. Chemokines, such as MCP1, attract macrophages into adipose tissue[81]. The infiltrated macrophages in the adipose tissue produce a wide array of pro-inflammatory cytokines, like TNF-α, IL-6, iNOS and IL-1β, which can impair insulin sensitivity[82]. In addition, saturated fatty acids can directly induce the expression of these inflammatory cytokines via the TLR4 and the NF-κB pathway[83]. Inhibition of hypothalamic IKKβ, which is induced by NF-κB, improves insulin and leptin sensitivity, preventing diet-induced obesity[84]. Mice with myeloid-TLR4 deletion are protected against high fat diet induced inflammation, adipose macrophage infiltration and IR[85]. To get an indication of the inflammation in the hypothalamus, the expression of a range of different inflammatory mediators was tested. However, the inflammatory mediators were not detectable. Only the pro-inflammatory cytokine TNF-α was detectable, but there no differences in expression found between the groups (fig. 17).

Another way to examine the inflammation in the hypothalamus is establish microglia infiltration and activation in the tissue. For this purpose, the expression of two microglial markers were measured: CD11b and CD68, which are commonly expressed on microglia[72] and can therefore be used as a marker of microglial infiltration. In addition, many studies have used mainly CD11b and CD68 as markers for microglial activation[86]. In the Lysm-PTP1B mice, the macrophages are lacking PTP1B and both CD11b and CD68 are also expressed on macrophages[87]. So the results might also include infiltrated macrophages from the blood. Both CD11b and CD68 are upregulated in KOHFD (fig. 18). The expectation was that both of the markers would be elevated in the WTHFD group and that the inhibition of PTP1B could restore the levels back to the level of the WTChow. However, the opposite seems to be true, the inhibition of PTP1B under HFD conditions leads to an increase in microglia activation in the hypothalamus. Inhibiting PTP1B in myeloid cells does not seem to be a good way to decrease inflammation in the hypothalamus. Hypothalamic inflammation does occur in response to HFD, in both rodents and humans[19] and could be an important mechanism responsible for the development of obesity and T2D. The role of microglia in this needs to be further investigated. Microglia are suggested to not be of importance in the acute inflammation in the first days after the initiation of the HFD, but accumulation and enlargement of microglia does occur later in the stage of the persisting inflammation[19]. The molecular link between obesity and inflammation, and the role of PTP1B therein, remains to be completely established.

4.6 PTP1B in ER-stress

Another important pathway indicated as possible link between high fat feeding and IR is the ER-stress pathway. Research has shown that prolonged high fat feeding leads to ER-stress, and this in turn contributes to the development of IR[10]. Neurons in the

hypothalamus expressing the LepR are exposed to ER-stress-associated factors such as increased FFAs and other nutrients, and it has been shown that ER-stress in the hypothalamus contributes to LR and, consecutively, to obesity[88]. Because of the potential role for PTP1B in decreasing ER-stress, through IRE1[12], several ER-stress markers were investigated. From the PERK-pathway, ATF4 levels were measured. The levels of both the un-spliced and the spliced XBP1 were measured from the IRE1-pathway. Also, levels of CHOP were measured, CHOP induces apoptosis in the cell in response to prolonged ER-stress. The increase of ATF4 in WTHFD (fig. 21) confirms the hypothesis that high fat feeding leads to ER-stress. However, $PTP1B^{-/-}$ is not able to lower ER-stress through ATF4, because the levels are not decreased in KOHFD. The same can be said about CHOP, it increases in WTHFD, but the levels are not decreased in KOHFD. From the difference in levels of XBP1t and XBP1s (fig. 22), the degree of splicing can be concluded. The level of total XBP1 does not increase in WTHFD, while the amount of spliced XBP1 increases. This indicates that splicing is increased in WTHFD. However, inhibition of PTP1B does not decrease the level of splicing back to normal. In conclusion, HFD does induce ER-stress through both the PERK and the IRE1 pathway, but mutation of myeloid PTP1B does not have an effect on the ER-stress. Yet, the levels of IRE1-mediated ER-stress are decreased in Lysm-PTP1B mice on chow diet (fig. 22). These results are in agreement with the HF-induced ER-stress through JNK and IRE1, found in Ozcan et al.[10], although PTP1B deletion is not able to reduce the ER-stress in HFD. The effect is only observed in mice on chow-diet, this could indicate that the HFD is too high in fat and sugar to have an effect and maybe a more moderate-fat diet would show an improvement. Liver specific deletion of PTP1B did attenuate diet-induced ER-stress[17]. So it could be that the deletion of PTP1B in myeloid cells just did not have an influence on the ER-stress in the hypothalamus.

Previous research has shown that obesity creates ER-stress and initiates the UPR signalling pathways in the hypothalamus, which, in turn, leads to inhibition of LepR signalling and creation of LR[88]. The translocation of the LepR to the membrane is not altered in ER-stress conditions[88], indicating that there is no defect in the LepR. The binding of leptin to the LepR even increases when ER-stress is occurring[88]. Also, ER-stress induced in the hypothalamus of lean mice creates a phenotype similar to that seen in the brain of the obese mice; infusion of tunicamycin into the third ventricle increases AgRP and NPY levels and blocks leptin-stimulated STAT3 activation[88]. Lysm-PTP1B mice have also shown to be protected against STAT3 induced inflammation[13]. Mice with the XBP1 gene knocked out in neurons show decreased leptin signalling, leading to leptin resistance[88]. Our WTHFD mice show increased splicing of XBP1. This could indicate that chronic ER-stress leads to exhaustion of the UPR, causing leptin resistance. Knocking out PTP1B in macrophages and myeloid microglia might not have the desired effect, because there are not enough myeloid microglia in the brain and the infiltrated macrophages do not have enough impact either.

4.7 Conclusion

In the current study, we showed that in the hypothalamus of diet-induced obese mice, there was no increase in PTP1B expression. Mutation of PTP1B in myeloid cells did reduce the increased levels of insulin and leptin, indicating that inhibiting myeloid PTP1B enhances insulin and leptin sensitivity. However, Lysm-PTP1B mice had no reduced adiposity and inflammation was not improved. The Lysm-PTP1B mice did show a decrease in ER-stress through the IRE1 pathway. This effect was, however, not observed in the Lysm-PTP1B mice on HFD.

In summary, myeloid PTP1B inhibition could be used in treatment against obesity and T2D because it improves insulin and leptin signalling. Inhibiting myeloid PTP1B does not seem to affect the inflammation in the hypothalamus. Inhibition of myeloid PTP1B could be used to reduce ER-stress in the hypothalamus, but it does not work in combination with HFD.

4.8 Future studies

In future studies, the effect of PTP1B on ER-stress can be extended, the ATF6 pathway has not yet been investigated. Also, the decrease in IRE1 mediated ER-stress in the hypothalamus of Lysm-PTP1B mice found in this study should be further investigated.

The effects of inhibiting myeloid PTP1B should be further investigated in future studies. The effect of the inhibition of myeloid PTP1B could be investigated in a primary microglia cell model. The microglia would have to be isolated from pups, so the HFD factor would be left out. On the other hand, LPS can be added to the cells to mimic the effects of HFD in microglia. Levels of different inflammatory factors can be measured from the medium of the cells using ELISA, mRNA can be measured using qPCR and Western blot can be used to measure levels of inflammatory proteins.

In future studies, difficulties that accompany microglia isolation could be avoided by studying the cells in stained brain slices[89]. Animals will be perfused before the cull and their brains will be stored at -80°C. The brains will be sliced and immunohistochemically stained for CD11b, CD39 and Iba1. Microglia phenotypes can be reconstructed using confocal microscopy and Iba1 staining[89]. Activated microglia, as seen in the inflammatory condition in high fat diet, will show a less branched phenotype taking up less surface. Individual cells can still be analysed and also quantified. In this way microglial activation can be analysed.

The brains that were collected from the mice in this study have been separated into hypothalamus, hippocampus and cortex. The hippocampus and cortex can still be investigated for levels of inflammation and ER-stress in forthcoming research. Also, microglia markers can be measured to get an idea of the microglia and macrophage infiltration there. Levels of inflammation and ER-stress in the hippocampus can be an important indication of effects that HFD may have on memory and cognition. Infiltration of microglia and upregulated neuroinflammation are associated with Alzheimer's

disease[24]. In addition, obesity has been linked with Alzheimer's disease, with hippocampal neuroinflammation as a possible underlying mechanism[90,91]. The number of people suffering from both obesity and Alzheimer's are expected to be increasing in the coming decades[91], that makes the link between the two an interesting target for future research.

Since the Lysm-PTP1B mice did not show a deletion of PTP1B in microglia, another way to investigate the role of PTP1B in microglia cells might be a more specific microglia knock-out model. Microglia are an important part of the mechanism behind many brain diseases and the role of PTP1B in microglia during obesity is a so far unexplored area.

The ultimate goal of the study is to find a cure for T2D and obesity and therefore clinical studies are necessary to test the effects of PTP1B inhibitors on humans. There are already clinical studies performed using PTP1B inhibitors, such as ertiprotafib[92], with varying results. More research is needed to understand the mechanism behind PTP1B in order to develop a suitable therapy against T2D and obesity.

Appendix A: List of abbreviations

ER	Endoplasmic reticulum
HFD	High fat diet
InsR	Insulin receptor
IR	Insulin resistance
KO	"Knock-out" mice are Lysm-PTP1B mice
KOChow	Knock-out mice on chow diet
KOHFD	Knock-out mice on high fat diet
LepR	Leptin receptor
LR	Leptin resistance
Lysm-PTP1B	Mice with the PTP1B gene knocked out of the myeloid cells
PTP1B	Protein tyrosine phosphatase 1B
PTP1B$^{fl/fl}$	Mice with the PTP1B gene floxed with two LoxPs
T2D	Type 2 diabetes
UPR	Unfolded protein response
WT	"Wild-type" mice are PTP1B$^{fl/fl}$ mice
WTChow	Wild-type mice on chow diet
WTHFD	Wild-type mice on high fat diet

Appendix B: Primer sequences

Gene	F/R	Sequence
NoNo	Forward	5'-GCCAGAATGAAGGCTTGACTAT
	Reverse	5'-TATCAGGGGGAAGATTGCCCA
PTP1B	Forward2	5'-ATGTCAGCCCTTTTGACCACA
	Reverse2	5'-GGGTGAGAATATAGCTCCTCTGG
NPY	Forward	5'-ATGCTAGGTAACAAGCGAATGG
	Reverse	5'-TGTCGCAGAGCGGAGTAGTAT
POMC	Forward	5'-GTGCCAGGACCTCACCACGG
	Reverse	5'-CGTTGCCAGGAAACACGGGC
MC4R	Forward	5'-CCCGGACGGAGGATGCTAT
	Reverse	5'-TCGCCACGATCACTAGAATGT
LepR	Forward	5'-TGGTCCCAGCAGCTATGGT
	Reverse	5'-ACCCAGAGAAGTTAGCACTGT
InsR	Forward	5'-AGACCAACTGTCCTGCCACT
	Reverse	5'-ACACACTTGGTGGGGTCATC
TNF-a	Forward	5'-CCCTCACACTCAGATCATCTTCT
	Reverse	5'-GCTACGACGTGGGCTACAG
iNOS	Forward	5'-GGAGTGACGGCAAACATGACT
	Reverse	5'-TAGCCAGCGTACCGGATGA
IL-6	Forward	5'-TAGTCCTTCCTACCCCAATTTCC
	Reverse	5'-TTGGTCCTTAGCCACTCCTTC
IL-1B	Forward	5'-GCAACTGTTCCTGAACTCAACT
	Reverse	5'-ATCTTTTGGGGTCCGTCAACT
IL-1a	Forward	5'-GCACCTTACACCTACCAGAGT
	Reverse	5'-AAACTTCTGCCTGACGAGCTT
IL-10	Forward	5'-GCTCTTACTGACTGGCATGAG
	Reverse	5'-CGCAGCTCTAGGAGCATGTG
GFAP	Forward	*Unknown*
	Reverse	*Unknown*
CD11b	Forward	5'-CCCCACACTAGCATCAAGGG
	Reverse	5'-GAGGCAAGGGACACACTGAC
CD68	Forward	5'-TGTCTGATCTTGCTAGGACCG
	Reverse	5'-GAGAGTAACGGCCTTTTTGTGA
Chop	Forward	5'-CTGCCTTTCACCTTGGAGAC
	Reverse	5'-CGTTTCCTGGGGATGAGATA
XBP1t	Forward	5'-AAGAACACGCTTGGGAATGG
	Reverse	5'-ACTCCCCTTGGCCTCCAC
XBP1s	Forward	5'-GAGTCCGCAGCAGGTG
	Reverse	5'-GTGTCAGAGTCCATGGGA
SOCS3	Forward	5'-ACCAGCGCCACTTCTTCACA
	Reverse	5'-GTGGAGCATCATACTGGTCC
ATF4	Forward	5'-ATGGCCGGCTATGGATGAT
	Reverse	5'-CGAAGTCAAACTCTTTCAGATCCAT

Appendix C: Experimental procedures

Appendix C.1: Microglia isolation

Always work sterile, and unless mentioned otherwise, work on ice.

1. Remove the brain from an adult mouse and place the brain in a 50 ml tube containing 5-10 ml of *medium A*
2. Keep the material on ice
3. Remove the meninges and brain stem with a pair of tweezers in a petri dish without medium, but on ice (put the petri dish on top of another petri dish filled with ice)
4. Brains without meninges immediately go into small amount of *medium A* on another petri dish (do not leave them to dry)
5. Cut the brain into small pieces with two scalpels no. 11
6. Pick up the minced brain with a little bit of *medium A* (about 400µl) with a blue tip, gently pipette up and down so the brain falls into small pieces
7. Collect the minced brain parts in a 50 ml tube with *medium A* (approx. 20 ml) and keep the tube on ice
8. After 3-5 min remove the *medium A* from the 50 ml tube (pipet by hand and not with aspirator)
9. Add 5 ml of *trypsin medium*
10. Put in the water bath (37°C) for 15 minutes
11. Shake the tube every couple of minutes (± 5 times)
12. Add 5 ml of *trypsin inhibition medium*
13. Leave for 3-5 minutes at room temperature (pellet will be going done)
14. Remove the *trypsin inhibition medium*
15. Wash with 5-10 ml of *wash medium*
16. Remove the excess *wash medium* (pipet by hand and not with aspirator) and leave around 1ml
17. Carefully, slowly triturate cells by pipetting them on a nylon mesh (70µm)
    Do not use too much force, otherwise you will destroy your cells
18. Add about 25 ml of *DMEM/FCS* and centrifuge for 10 minutes at 1500 rpm at 12°C
19. Remove the supernatant and add 1 ml of *DMEM/FCS*
20. Resuspend with small (but not to small) pipette tip (carefully and slowly!)
21. Add 9 ml DMEM/FCS into a 75 cm^2 flask
22. Add the 1 ml of cell suspension to the flask
23. Gently swerve
24. Put the flasks in the incubator (37°C and 5% CO_2)

After 2 days

25. Warm up your fresh medium until it's about 37°C
26. Remove the old medium from the flasks into 50 ml tubes
27. Add 9 ml of fresh *DMEM/FCS* to each flask
28. Put the flasks back into the incubator
29. Centrifuge tubes (5 min, 3000 rpm)
30. After the centrifugation of 'old' medium, collect the supernatant and ad 6 ml of it to each flask

Change half of the medium every time you are shaking off microglia

There should be a confluent layer of astrocytes around 5 to 7 days (very variable)

After 7 - 10 days you can harvest microglia (variable, you should shake when you see a lot of floating microglia in the medium)

Shaking microglia

31. 3-4 hours shaking in a 37°C room 150 rpm **alternatively:** hand-shaking (about 30 circles movements)
32. No centrifuging
33. Collect the supernatant and put 2 ml per well on 24-well plate
34. Repeat 2-3 times (with the 1,5-2h intervals) until the cells on the multi-well plate will be confluent
35. Change the medium for fresh 10% DMEM after 1-1,5 h (when the cells will attach)

Preparation media

DMEM/FCS	***500 ml***	***final concentration***
FCS [3] (100 %)	50 ml	10 %
Sodium Pyruvate [4] (100 mM)	5 ml	1 mM
Pen/strepto [2]	2.5 ml	
L-glutamine	5 ml	
DMEM [5]	435 ml	-

Medium A *(make 2-3 tubes)*	***50 ml***	***final concentration***
HBSS [6]	48.1 ml	-
Glucose 45 % [7]	650 µl	0.585 %
HEPES 1M [8]	750 µl	15 mM
Pen/Strep [2] (10000 units/ml Penicillin/	500 µl	100 units/ml Penicillin
10000 µg/ml Streptomycin)		100 µg/ml Streptomycin

Trypsin medium	***15 ml***	***final concentration***
2.5 % Trypsin [9]	1.5 ml	0,25 %
DNase I [10] 100x (100000 U/ml)	150 µl	1 x (1000 U/ml)
Medium A	13.5 ml	-

Trypsin inhibition medium	***15 ml***	***final concentration***
Medium A	12 ml	-
FCS [3] (100 %)	3 ml	20 %
DNase I [10] 100 x (100000 U/ml)	150 µl	1x (1000 U/ml)
Trypsin inhibitor [11] (10 mg/ml)	150 µl	0.1 mg/ml

Wash medium	***30 ml***	***final concentration***
Medium A	27 ml	-
FCS [3] (100 %)	3 ml	10 %
DNase I [10] 100 x (100000 U/ml)	300 µl	1x (1000 U/ml)

Materials

- Culture Flasks, 75 cm^2 or 25 cm^2 Greiner Bio-one, catalogue number 658 170
- 50 ml tubes
- Petri dishes
- 2 no 11 scalpels
- Scissors
- Tweezers (flat and pinched)
- Container with ice
- Nylon meshes (70µm)
- P1000 pipette + tips, pipette-boy + pipettes (5, 10 and 25 ml)

- Cell culture hood
- Water bath (37°C)
- Incubator (37°c)
- Centrifuge

Solutions

1. FBS, Gold, PAA, catalogue number A15-151
2. Penicillin-Streptomycin Solution, Gibco, catalogue number 15140-122
3. L-Glutamine (100x), Gibco, catalogue number 25030-024
4. Sodium Pyruvate, Gibco, catalogue number 11360-039
5. DMEM (1x) liquid, Life Technologies, catalogue number 41965-039
6. HBSS (1x) liquid, Gibco, catalogue number 14170-088
7. D-(+)-Glucose solution 45%, Sigma-Aldrich, catalogue number G8769
8. HEPES 1M, Gibco, catalogue number 15630-056
9. Trypsin, Gibco, catalogue number 15090-046
10. DNase I, Roche, catalogue number 104159
11. Trypsin inhibitor, Sigma-Aldrich, catalogue number T6522
12. Ethanol (70%)

Appendix C.2: Western blot protocol

Collecting samples

1. Add 200µl Protease inhibitor cocktail solution (cOmplete: 11836145001) and 100µl vandadate (made up in tube) to 10 ml RIPA buffer (made by Louise Grant)

WORK ON ICE!

2. Aspirate medium from the seeded and treated 96-well plate (with pump)
3. Wash all wells 2x with ice-cold PBS
4. After 2nd wash, make sure all PBS is out!
5. Add RIPA lysis buffer to each well (1ml/10cm^2)
6. Incubate for 5 minutes
7. Pipette up and down and scrape with cell scraper (or use pipette tip in small wells)
8. Collect cells eppendorfs and put on ice
9. Centrifuge for 10 min, 10.000g, 4°C
10. Collect the supernatant in new eppendorfs
11. Optionally store at -20°C, otherwise continue with BCA

BCA (Using Pierce BCA protein assay kit, Thermoscientific: 23227)

12. Add 5µl of each sample (and standard) to each well of the 96-well plate in duplo
13. Mix 196µl Reagent A with 4µl Reagent B for each well
14. Add 200µl of Reagent mix to each well (multichannel)
15. Incubate for 30 minutes
16. Read plate at 562nm using platereader (Versa Max, Molecular Devices)

Western blot

17. Make up loading buffer:
    a. 100µl SDS loading buffer 5x (made by Nicola Morrice)
    b. 5µl BME (mercapto-2-ethanol, Fisher: M/p200/05)
18. Add loading buffer to sample (1:5)
19. In 95□C heating block for 10 minutes
20. Store in -20□C or continue with Western blot
21. Vortex samples briefly (and spin down)
22. Prepare running buffer:
    a. MOPS buffer filled up with dH_2O (1:20) (make 500 ml for 2 gels)
23. Prepare gels
24. Load ladders
25. Load samples (write down in what order)
26. Run at 60 Volt for about 20 minutes (until a clear front appears), then run at 130 Volt for 80 minutes
27. Prepare transfer buffer while gel is running:
    a. 200ml 10x Tris-Glycine
    b. 400ml Methanol (Sigma, 32213)
    c. 1400ml dH_2O
    d. Store in 4□C
28. Prepare membrane and filters (cut all 15 by 8 cm)
29. Put gel in transfer buffer

30. Soak sponges, filters and membrane in transfer buffer
31. Make 'sandwich': Sponge - 2 filters – membrane – gel – 2 filters → roll out bubbles
32. Make sure the gel is the right way around
33. Close sandwhich, put in machine (opposite colours), add magnetic stirrer and iceblock
34. Fill up with transfer buffer
35. Run on magnetic stirrer for 1 hour at 100 Volt
36. Membrane in Ponceau for 1 minute
37. Wash with dH_2O
38. Make photo of membrane

Primary antibody

39. Wash in TBS-T (2x5 min.) (cut membrane if necessary)
40. Block with TBS-T + 5% Milk for 1 hour
41. Wash in TBS-T (2x5 min.)
42. Prepareprimary antibody in TBS-T + 2% BSA
43. Add antibody solution and membrane in a bag and seal
44. Leave overnight (weekend) in 4°C

Secondary antibody

45. Antibody can be re-used
46. Wash (3x10min.) with TBS-T
47. Prepare secondary antibody (1:5000) in TBS-T + 5% milk
48. Incubate withsecondary antibody for 1 hour on rocker at room temperature
49. Wash (3x10min.) with TBS-T
50. Dry membrane slightly and carefully on paper towel
51. Expose membrane using ECL mix (50:50, ECL1 and ECL2) for 1 minute
    a. Pierce ECL: 32209
52. Take pictures
53. Wash in TBS-T (2x5 min.)
54. Do another staining or store in TBS-T in 4°C for later re-use

Appendix C.3: Flow cytometry protocol for primary microglia

Cell collection

1. Collect media in tube
2. Wash with PBS (Gibco: 14190-094) twice → add to media
3. Detach cells with 3ml Accutase (Gibco: A11105-01) for 10 minutes
4. Wash with PBS → add to media
5. Spin at 2500g, 5mins
6. Resuspend in 0,5 ml PBS

Blocking

7. 100µl in each well *(5 wells: 1 sample, 3 single stains, 1 non-stained ctrl)*
8. Make blocking-AB mix:
    a. 1 µl blocking-AB per well
    b. Dilute 1*(number of wells + a bit extra) blocking-AB in PBS (1:100)
        i. Blocking AB: BD 553141 (07692)
9. Add 50µl of blocking AB mix to each sample
10. Incubate for 10 minutes

Antibody staining

11. Add 150µl PBS
12. Centrifuge plate (2000rpm, 5 min) (+balance!)
13. Throw out liquid in the sink
14. Make antibody mix by adding the right amount of each AB to 200µl PBS

Protein	**Anitbody**	**Dilution***	**Amount (µl)**	
F4/80	AF 700	200x	1	Rat anti mouse
CD11b	PE-CF594 (Texas red)	200x	1	BD Biosciences 562287 (lot: 3128600)
CD45	PE	200x	1	BD Biosciences 553089 (lot: 19521)

**Dilution corrected for the 30 µl that will stay behind in the well*

15. Throw liquid out of the plate (about 30µl will stay behind in each well)
16. Add 50 µl of mix to the sample well
17. Add 50 µl of PBS to the SS wells and add 1 µl of each antibody to the right well
18. Add 200 µl of PBS to the non-stained sample well
19. Plate lay-out:

	1	**2**	**3**
A	Sample		
B	Single stain F4/80	Single stain CD11b	Single stain CD45
C	Non-stained control		

20. Incubate for 1,5 hours in the dark

Single staining: beads

21. Add 1 ml of PBS to a FACS-tube for each of the coloured antibodies (label the tubes)
22. Add 1 drop of positive plastic beads *(BD 51-90-9000949, lot: 28890)*
23. Add 1 µl of each coloured antibody to the right tube
24. Vortex the tubes
25. **Incubate 1,5 hours in the dark**
26. Spin the tubes (max speed, 10 mins)
27. Resuspend pellet (beads) in 1 ml PBS and leave in the dark
28. Add negative control beads *(BD 51-90-9001291, lot: 28890)*

Transfer cells to tubes

29. Wash wells with 150 µl PBS, centrifuge plate (2000rpm, 5 min) and throw out liquid
30. Wash again with 150 µl PBS, centrifuge plate (2000rpm, 5 min) and throw out liquid
31. Add 100µl PBS and transfer cells to FACS-tubes
32. Add 400µl of PBS to the tubes
33. Keep in the dark

Flow cytometry

All tubes etc. on ice and in the dark
Turn on machine 15 minutes before to warm up the lasers (if not on)
Sheeth fluid must be enough; waste must not be too full

34. Flush machine with dH_2O
35. Create compensation controls (delete rest, or put to 0)
36. Then start with measuring (always vortex first, when it takes long: vortex again)
37. First: non-stained control (set machine on: low) → record
38. Adjust voltage parameter of (all) lasers
39. Stopping gate: 10.000 events
    Storing gate: all events
40. Next: single stains
41. Check if overlap (%) is not too high of the ones you are using
42. Compensation
43. Start with samples (record data)
44. First sample:
    a. Graph: FSC vs. SSC → select gate: *live cells*
    b. New graph: Plot the two markers of DCs → select gate*: positive cells*, so the population with both parameters high
    c. Make 5 other graphs for the other markers
45. Run all samples through the machine
46. Afterwards: clean the machine
    a. Run a tube of FACS-clean through the machine (handle to the side)
    b. Run a tube of FACS-rinse through the machine
    c. Put a tube of H2O in the machine
    d. *Aquire data* to check if machine is properly cleaned
47. Press *Standby* and *Lo*
48. Export all FCS files to your location (check if amount of files is correct)

Appendix C.4: RNA isolation

Trizol and chloroform: work in hood

1. Add Tri-Reagent (10 µl/mg tissue)
2. Homogenize tissue with tissue-homogenizer (wash/dry after each sample)
3. Incubate 5-10 min RT
   Optionally store at –80°C, otherwise continue with phase separation

Phase separation

4. Thaw frozen Trizol samples at room temperature
5. Add 200 µl chloroform per 1 ml of Tri-Reagent
6. Vortex briefly
7. Leave 15 min at RT
8. Spin 15 min at 12000 g and 4°C
9. Carefully aspirate the upper aqueous phase containing the RNA and transfer to fresh (RNase-free) 1.5 ml tube (do not touch the interphase with the pipet tip)

RNA precipitation

10. Add 500 µl of isopropanol per 1 ml of Tri-Reagent used for the initial homogenization
11. Vortex briefly
12. Store at -20°C overnight (for cleaner RNA)

Day 2

13. Spin 15 min at 12000 g and 4°C
14. Carefully aspirate supernatant by decanting
15. Wash pellet twice:
    a. Add 75% ethanol (RNase free) to pellet
    b. Spin 5 min at 7600 g and 4°C
    c. Aspirate supernatant by decanting
16. Briefly spin down remaining ethanol
17. Remove remaining ethanol by pipetting using a sharp tip
18. Air dry pellet for 1-5 min until it has a slightly transparent glazy appearance (not dry out!)
19. Dissolve in TE-buffer (20 µl) → on ice!

RNA quantification

20. Nanodrop machine: DNA: 260/280
21. First blank (dH_2O), then samples
22. Optionally store in -20°C, otherwise continue with cDNA synthesis

Materials

Tri-reagent (Sigma: T924)
Chloroform (Sigma: C2432)
Tris-EDTA (TE) Buffer Solution (Fluka: 93302)

Appendix C.5: Complementary DNA synthesis form RNA

Additional information on protocol Tetro cDNA synthesis kit (Bioline: BIO-65043), as used in Delibegovic's lab

Keep the kit and the RNA samples on ice!
Leave Reverse Transcriptase and RNase Inhibitor in -20□C until it is needed

1. Put correct amount of nuclease-free water in each tube (amounts calculated from protein quantification)
2. Add correct amounts of each RNA sample to the tubes (amounts calculated from protein quantification)
3. Make mastermix, following manufacturer's instructions
    - For primers: Use Oligo $(dT)_{18}$: Random Hexamer 50:50
4. Make mastermix without Reverse Transcriptase (for "-RT controls")
5. Add mastermix (8µl) to the samples
6. Run "Tetro synthesis" protocol on Thermocycler (Bio-Rad T100)
7. Dilute 15µl of each sample into 135µl dH_2O (Gibco: 10977-035)
8. Take the 5µl left-over of each sample into one tube
    - Take 30 µl of the sample mix into 120µl dH_2O →standard 1
    - Take 15 µl into 135µl of dH_2O → standard 2
    - Take 15 µl into 135µl of dH_2O → standard 3
    - Take 15 µl into 135µl of dH_2O → standard 4

Appendix C.6: Quantitative PCR protocol (work on ice)

Prepare mastermixes

1. Mix forward/reverse primers (50/50): 50 µl of each (aliquots in freezer)
2. 384 well plate: Mark where you will put the different genes/samples/standards/controls
3. 10µl reaction mix per well, so 8 µl Mastermix per well:
    - 5µl go- Taq qPCR master mix (Promega: A600A)
    - 2.5µl nuclease free water (Promega: P119E)
    - 0.5µl forward and reverse primers (See primer list in appendix B)
4. Make a mastermix for each gene:
   Each sample in triplicate for each gene that you are looking at
   Standard curve for each gene to check the primer efficiency (4 concentrations)
   4 control wells for each gene
   Mastermix for each gene: *number of samples**3 + 4*3 + 4 + *a bit extra*
   First water, then primers, then Taq

Plate-up

5. 8µl of the reaction master mix per well
6. 3*2µl of the appropriated cDNA sample
7. 2*2µl of –RT sample for each gene
8. 2*2µl of nuclease free water for each gene as a no template control (NTC) controls for
9. 3*2µl of the 4 standards (serial dilution) to get the standard curve (triplicate)
10. Briefly spin plate down at 4°C (balance!)
11. Optionally leave the plate in 4°C overnight
12. qPCR machine (Roche 480) in room 4.55
    - LightCycler 480 software 1.5.0
    - Sybr- green I 384 program
    - Correct volume (10µl)
    - Run (about 1 hour)

Analysis

13. When machine is finished: navigator-experiments-export (copy to USB)
14. For analysis in LightCycler:
    - Import
    - TM calling
        i. Sybr green I
        ii. Calculate
        iii. Check controls
    - Abs quant/2nd deriv. max:
        i. High sensitivity→calculate
        ii. Select all→ export table
        iii. Check controls
        iv. Check for outliers
        v. Select standards → standard curve (replicates: 3, initial concentration: 1, dilution factor: 10) → calculate
        vi. Note slopes of genes (should be -3.3 with a standard deviation of 0.3)
15. Cp values → Excel:
    - Efficiency=$10^{(-1/slope)}$
    - y=Efficieny$^{(average\ of\ control\ Cp's/Cpx)}$
    - relative gene expression=$y_{gene}/y_{housekeeping}$
    - relative fold change in gene expression= relative gene expression /average of controls

Bibliography

1. Smyth S, Heron A. Diabetes and obesity: The twin epidemics. *Nat Med*. 2006;12(1):75-80.

2. Haslam DW, James WPT. Obesity. *The Lancet*. 2005;366(9492):1197-1209.

3. Ng M, Fleming T, Robinson M, et al. Global, regional, and national prevalence of overweight and obesity in children and adults during 1980–2013: A systematic analysis for the global burden of disease study 2013. *The Lancet*. 2014.

4. Kelly T, Yang W, Chen C, Reynolds K, He J. Global burden of obesity in 2005 and projections to 2030. *Int J Obes*. 2008;32(9):1431-1437.

5. Schwartz MW, Porte D,Jr. Diabetes, obesity, and the brain. *Science*. 2005;307(5708):375-379.

6. Velloso L, Schwartz M. Altered hypothalamic function in diet-induced obesity. *Int J Obes*. 2011;35(12):1455-1465.

7. Bruning JC, Gautam D, Burks DJ, et al. Role of brain insulin receptor in control of body weight and reproduction. *Science*. 2000;289(5487):2122-2125.

8. Balthasar N, Coppari R, McMinn J, et al. Leptin receptor signaling in POMC neurons is required for normal body weght homeostasis. *Neuron*. 2004;42(6):983-991.

9. Weissmann L, Quaresma PG, Santos AC, et al. IKKepsilon is key to induction of insulin resistance in the hypothalamus, and its inhibition reverses obesity. *Diabetes*. 2014;63(10):3334-3345.

10. Ozcan U, Cao Q, Yilmaz E, et al. Endoplasmic reticulum stress links obesity, insulin action, and type 2 diabetes. *Science*. 2004;306(5695):457-461.

11. Bence KK, Delibegovic M, Xue B, et al. Neuronal PTP1B regulates body weight, adiposity and leptin action. *Nat Med*. 2006;12(8):917-924.

12. Gu F, Nguyen DT, Stuible M, Dube N, Tremblay ML, Chevet E. Protein-tyrosine phosphatase 1B potentiates IRE1 signaling during endoplasmic reticulum stress. *J Biol Chem*. 2004;279(48):49689-49693.

13. Grant L, Shearer K, Czopek A, et al. Myeloid-cell protein tyrosine phosphatase-1B deficiency in mice protects against high-fat diet and lipopolysaccharide induced inflammation, hyperinsulinemia and endotoxemia through an IL10 STAT3 dependent mechanism. *Diabetes*. 2013:DB_130885.

14. Klaman LD, Boss O, Peroni OD, et al. Increased energy expenditure, decreased adiposity, and tissue-specific insulin sensitivity in protein-tyrosine phosphatase 1B-deficient mice. *Mol Cell Biol*. 2000;20(15):5479-5489.

15. Elchebly M, Payette P, Michaliszyn E, et al. Increased insulin sensitivity and obesity resistance in mice lacking the protein tyrosine phosphatase-1B gene. *Science*. 1999;283(5407):1544-1548.

16. Delibegovic M, Bence KK, Mody N, et al. Improved glucose homeostasis in mice with muscle-specific deletion of protein-tyrosine phosphatase 1B. *Mol Cell Biol*. 2007;27(21):7727-7734.

17. Delibegovic M, Zimmer D, Kauffman C, et al. Liver-specific deletion of protein-tyrosine phosphatase 1B (PTP1B) improves metabolic syndrome and attenuates diet-induced endoplasmic reticulum stress. *Diabetes*. 2009;58(3):590-599.

18. Owen C, Czopek A, Agouni A, et al. Adipocyte-specific protein tyrosine phosphatase 1B deletion increases lipogenesis, adipocyte cell size and is a minor regulator of glucose homeostasis. *PLoS One*. 2012;7(2):e32700.

19. Thaler JP, Yi CX, Schur EA, et al. Obesity is associated with hypothalamic injury in rodents and humans. *J Clin Invest*. 2012;122(1):153-162.

20. Zabolotny JM, Bence-Hanulec KK, Stricker-Krongrad A, et al. PTP1B regulates leptin signal transduction in vivo. *Developmental cell*. 2002;2(4):489-495.

21. Nakagawa Y, Chiba K. Diversity and plasticity of microglial cells in psychiatric and neurological disorders. *Pharmacol Ther*. 2015.

22. Minghetti L, Levi G. Microglia as effector cells in brain damage and repair: Focus on prostanoids and nitric oxide. *Prog Neurobiol*. 1998;54(1):99-125.

23. Hirsch EC, Hunot S. Neuroinflammation in parkinson's disease: A target for neuroprotection? *Lancet neurology*. 2009;8(4):382-397.

24. Maccioni RB, Rojo LE, Fernandez JA, Kuljis RO. The role of neuroimmunomodulation in alzheimer's disease. *Ann N Y Acad Sci*. 2009;1153(1):240-246.

25. Grigoriadis N FAU - Grigoriadis,Savas, Grigoriadis S FAU - Polyzoidou,Eleni, Polyzoidou E FAU - Milonas,Ioannis, Milonas I FAU - Karussis,Dimitrios, Karussis D. Neuroinflammation in multiple sclerosis: Evidence for autoimmune dysregulation, not simple autoimmune reaction. . (0303-8467 (Print); 0303-8467 (Linking)).

26. Dobos N, de Vries EFJ, Kema IP, et al. The role of indoleamine 2,3-dioxygenase in a mouse model of neuroinflammation-induced depression. *J Alzheimer's Dis*. 2012;28(4):905-915.

27. Bear MF, Connors BW, Paradiso MA. *Neuroscience.* Vol 2. Lippincott Williams & Wilkins; 2007.

28. Bluestone JA, Herold K, Eisenbarth G. Genetics, pathogenesis and clinical interventions in type [thinsp] 1 diabetes. *Nature*. 2010;464(7293):1293-1300.

29. Fleming JW, Fleming LW, Davis CS. Fixed-dose combinations in type 2 diabetes–role of the canagliflozin metformin combination. *Diabetes, metabolic syndrome and obesity: targets and therapy*. 2015;8:287.

30. Li X, Song D, Leng SX. Link between type 2 diabetes and alzheimer's disease: From epidemiology to mechanism and treatment. *Clinical interventions in aging*. 2015;10:549.

31. Stefan N, Kantartzis K, Machann J, et al. Identification and characterization of metabolically benign obesity in humans. *Arch Intern Med*. 2008;168(15):1609-1616.

32. Pouliot MC, Despres JP, Nadeau A, et al. Visceral obesity in men. associations with glucose tolerance, plasma insulin, and lipoprotein levels. *Diabetes*. 1992;41(7):826-834.

33. Harris MI, Eastman RC. Early detection of undiagnosed diabetes mellitus: A US perspective. *Diabetes Metab Res*. 2000;16(4):230-236.

34. Dominguez R, Pagano M, Marschoff E, González S, Repetto M, Serra J. Alzheimer disease and cognitive impairment associated with diabetes mellitus type 2: Associations and a hypothesis. *Neurología (English Edition)*. 2014;29(9):567-572.

35. Johnson TO, Ermolieff J, Jirousek MR. Protein tyrosine phosphatase 1B inhibitors for diabetes. *Nature Reviews Drug Discovery*. 2002;1(9):696-709.

36. Tamrakar AK, Maurya CK, Rai AK. PTP1B inhibitors for type 2 diabetes treatment: A patent review (2011-2014). *Expert opinion on therapeutic patents*. 2014;24(10):1101-1115.

37. He Y, Yan H, Dong H, et al. Structural basis of interaction between protein tyrosine phosphatase PCP-2 and β-catenin. *Science in China Series C: Life Sciences*. 2005;48(2):163-167.

38. Combs AP. Recent advances in the discovery of competitive protein tyrosine phosphatase 1B inhibitors for the treatment of diabetes, obesity, and cancer. *J Med Chem*. 2009;53(6):2333-2344.

39. Koch L, Wunderlich FT, Seibler J, et al. Central insulin action regulates peripheral glucose and fat metabolism in mice. *J Clin Invest*. 2008;118(6):2132-2147.

40. Baskin DG, Wilcox BJ, Figlewicz DP, Dorsa DM. Insulin and insulin-like growth factors in the CNS. *Trends Neurosci*. 1988;11(3):107-111.

41. Baura GD, Foster DM, Porte D,Jr, et al. Saturable transport of insulin from plasma into the central nervous system of dogs in vivo. A mechanism for regulated insulin delivery to the brain. *J Clin Invest*. 1993;92(4):1824-1830.

42. Woods SC, Lotter EC, McKay LD, Porte D. Chronic intracerebroventricular infusion of insulin reduces food intake and body weight of baboons. . 1979.

43. Banks WA, Jaspan JB, Kastin AJ. Selective, physiological transport of insulin across the blood-brain barrier: Novel demonstration by species-specific radioimmunoassays. *Peptides*. 1997;18(8):1257-1262.

44. Steculorum SM, Solas M, Brüning JC. The paradox of neuronal insulin action and resistance in the development of aging-associated diseases. *Alzheimer's & Dementia*. 2014;10(1):S3-S11.

45. Cheatham B, Kahn CR. Insulin action and the insulin signaling network*. *Endocr Rev*. 1995;16(2):117-142.

46. Bryant NJ, Govers R, James DE. Regulated transport of the glucose transporter GLUT4. *Nature reviews Molecular cell biology*. 2002;3(4):267-277.

47. Klein S, Coppack SW, Mohamed-Ali V, Landt M. Adipose tissue leptin production and plasma leptin kinetics in humans. *Diabetes*. 1996;45(7):984-987.

48. Brennan AM, Mantzoros CS. Drug insight: The role of leptin in human physiology and pathophysiology—emerging clinical applications. *Nature clinical practice Endocrinology & metabolism*. 2006;2(6):318-327.

49. Münzberg H, Björnholm M, Bates S, Myers Jr M. Leptin receptor action and mechanisms of leptin resistance. *Cellular and Molecular Life Sciences*. 2005;62(6):642-652.

50. Xu AW, Kaelin CB, Takeda K, Akira S, Schwartz MW, Barsh GS. PI3K integrates the action of insulin and leptin on hypothalamic neurons. *J Clin Invest*. 2005;115(4):951-958.

51. Bjorbaek C, Buchholz RM, Davis SM, et al. Divergent roles of SHP-2 in ERK activation by leptin receptors. *J Biol Chem*. 2001;276(7):4747-4755.

52. Bates SH, Stearns WH, Dundon TA, et al. STAT3 signalling is required for leptin regulation of energy balance but not reproduction. *Nature*. 2003;421(6925):856-859.

53. Pan H, Guo J, Su Z. Advances in understanding the interrelations between leptin resistance and obesity. *Physiol Behav*. 2014;130:157-169.

54. Considine RV, Sinha MK, Heiman ML, et al. Serum immunoreactive-leptin concentrations in normal-weight and obese humans. *N Engl J Med*. 1996;334(5):292-295.

55. Campfield LA, Smith FJ, Guisez Y, Devos R, Burn P. Recombinant mouse OB protein: Evidence for a peripheral signal linking adiposity and central neural networks. *Science*. 1995;269(5223):546-549.

56. Schwartz MW, Woods SC, Porte D, Seeley RJ, Baskin DG. Central nervous system control of food intake. *Nature*. 2000;404(6778):661-671.

57. Caro JF, Kolaczynski JW, Nyce MR, et al. Decreased cerebrospinal-fluid/serum leptin ratio in obesity: A possible mechanism for leptin resistance. *The Lancet*. 1996;348(9021):159-161.

58. Bjørbæk C, Elmquist JK, Frantz JD, Shoelson SE, Flier JS. Identification of SOCS-3 as a potential mediator of central leptin resistance. *Mol Cell*. 1998;1(4):619-625.

59. Glenn Stanley B, Kyrkouli SE, Lampert S, Leibowitz SF. Neuropeptide Y chronically injected into the hypothalamus: A powerful neurochemical inducer of hyperphagia and obesity. *Peptides*. 1986;7(6):1189-1192.

60. Cone RD, Lu D, Koppula S, et al. The melanocortin receptors: Agonists, antagonists, and the hormonal control of pigmentation. *Recent Prog Horm Res*. 1996;51:287-317; discussion 318.

61. Cai D. Neuroinflammation and neurodegeneration in overnutrition-induced diseases. *Trends in Endocrinology & Metabolism*. 2013;24(1):40-47.

62. Thaler JP, Schwartz MW. Minireview: Inflammation and obesity pathogenesis: The hypothalamus heats up. *Endocrinology*. 2010;151(9):4109-4115.

63. Heinonen KM, Dubé N, Bourdeau A, Lapp WS, Tremblay ML. Protein tyrosine phosphatase 1B negatively regulates macrophage development through CSF-1 signaling. *Proc Natl Acad Sci U S A*. 2006;103(8):2776-2781.

64. Xu H, An H, Hou J, et al. Phosphatase PTP1B negatively regulates MyD88-and TRIF-dependent proinflammatory cytokine and type I interferon production in TLR-triggered macrophages. *Mol Immunol*. 2008;45(13):3545-3552.

65. Schindler C, Levy DE, Decker T. JAK-STAT signaling: From interferons to cytokines. *J Biol Chem*. 2007;282(28):20059-20063.

66. Myers MP, Andersen JN, Cheng A, et al. TYK2 and JAK2 are substrates of protein-tyrosine phosphatase 1B. *J Biol Chem*. 2001;276(51):47771-47774.

67. van Exel E, Gussekloo J, de Craen AJ, et al. Low production capacity of interleukin-10 associates with the metabolic syndrome and type 2 diabetes : The leiden 85-plus study. *Diabetes*. 2002;51(4):1088-1092.

68. Abdelali A, Nimesh M, Carl O, et al. Liver-specific deletion of protein tyrosine phosphatase (PTP) 1B improves obesity-and pharmacologically induced endoplasmic reticulum stress. *Biochem J*. 2011;438(2):369-378.

69. Schröder M, Kaufman RJ. ER stress and the unfolded protein response. *Mutation Research/Fundamental and Molecular Mechanisms of Mutagenesis*. 2005;569(1):29-63.

70. Schönthal AH. Endoplasmic reticulum stress: Its role in disease and novel prospects for therapy. *Scientifica*. 2012;2012.

71. Matthews D, Hosker J, Rudenski A, Naylor B, Treacher D, Turner R. Homeostasis model assessment: Insulin resistance and β-cell function from fasting plasma glucose and insulin concentrations in man. *Diabetologia*. 1985;28(7):412-419.

72. Prinz M, Priller J, Sisodia SS, Ransohoff RM. Heterogeneity of CNS myeloid cells and their roles in neurodegeneration. *Nat Neurosci*. 2011;14(10):1227-1235.

73. Lee J, Tansey MG. Microglia isolation from adult mouse brain. In: *Microglia.* Springer; 2013:17-23.

74. Nikodemova M, Watters JJ. Efficient isolation of live microglia with preserved phenotypes from adult mouse brain. *J Neuroinflammation*. 2012;9(1):147.

75. Lee B, Lee J. Cellular and molecular players in adipose tissue inflammation in the development of obesity-induced insulin resistance. *Biochimica et Biophysica Acta (BBA)-Molecular Basis of Disease*. 2014;1842(3):446-462.

76. Friedman JM, Halaas JL. Leptin and the regulation of body weight in mammals. *Nature*. 1998;395(6704):763-770.

77. Erickson JC, Hollopeter G, Palmiter RD. Attenuation of the obesity syndrome of ob/ob mice by the loss of neuropeptide Y. *Science*. 1996;274(5293):1704-1707.

78. Huszar D, Lynch CA, Fairchild-Huntress V, et al. Targeted disruption of the melanocortin-4 receptor results in obesity in mice. *Cell*. 1997;88(1):131-141.

79. Banno R, Zimmer D, De Jonghe BC, et al. PTP1B and SHP2 in POMC neurons reciprocally regulate energy balance in mice. *J Clin Invest*. 2010;120(3):720-734.

80. Weisberg SP, McCann D, Desai M, Rosenbaum M, Leibel RL, Ferrante AW,Jr. Obesity is associated with macrophage accumulation in adipose tissue. *J Clin Invest*. 2003;112(12):1796-1808.

81. Chen A, Mumick S, Zhang C, et al. Diet induction of monocyte chemoattractant protein-1 and its impact on obesity. *Obes Res*. 2005;13(8):1311-1320.

82. Jager J, Grémeaux T, Cormont M, Le Marchand-Brustel Y, Tanti J. Interleukin-1β-induced insulin resistance in adipocytes through down-regulation of insulin receptor substrate-1 expression. *Endocrinology*. 2007;148(1):241-251.

83. Shi H, Kokoeva MV, Inouye K, Tzameli I, Yin H, Flier JS. TLR4 links innate immunity and fatty acid-induced insulin resistance. *J Clin Invest*. 2006;116(11):3015-3025.

84. Zhang X, Zhang G, Zhang H, Karin M, Bai H, Cai D. Hypothalamic IKKβ/NF-κB and ER stress link overnutrition to energy imbalance and obesity. *Cell*. 2008;135(1):61-73.

85. Saberi M, Woods N, de Luca C, et al. Hematopoietic cell-specific deletion of toll-like receptor 4 ameliorates hepatic and adipose tissue insulin resistance in high-fat-fed mice. *Cell metabolism*. 2009;10(5):419-429.

86. Hoogland IC, Houbolt C, van Westerloo DJ, van Gool WA, van de Beek D. Systemic inflammation and microglial activation: Systematic review of animal experiments. *J Neuroinflammation*. 2015;12:114-015-0332-6.

87. Chan W, Kohsaka S, Rezaie P. The origin and cell lineage of microglia—new concepts. *Brain Res Rev*. 2007;53(2):344-354.

88. Ozcan L, Ergin AS, Lu A, et al. Endoplasmic reticulum stress plays a central role in development of leptin resistance. *Cell metabolism*. 2009;9(1):35-51.

89. Baron R, Babcock AA, Nemirovsky A, Finsen B, Monsonego A. Accelerated microglial pathology is associated with aβ plaques in mouse models of alzheimer's disease. *Aging cell*. 2014;13(4):584-595.

90. Heneka MT, Carson MJ, El Khoury J, et al. Neuroinflammation in alzheimer's disease. *The Lancet Neurology*. 2015;14(4):388-405.

91. Tucsek Z, Toth P, Sosnowska D, et al. Obesity in aging exacerbates blood-brain barrier disruption, neuroinflammation, and oxidative stress in the mouse hippocampus: Effects on expression of genes involved in beta-amyloid generation and alzheimer's disease. *J Gerontol A Biol Sci Med Sci*. 2014;69(10):1212-1226.

92. Liu J, Zhang S, Nie F, et al. Discovery of novel PTP1B inhibitors via pharmacophore-oriented scaffold hopping from ertiprotafib. *Bioorg Med Chem Lett*. 2013;23(23):6217-6222.